tein: $n=5$; $P=0.517$). No clinical symptoms were detected in the biotin-deficient mice, and no significant differences of body weights were detected between biotin-sufficient and -deficient mice (data not shown). A significant ($P<0.01$) increase of the serum TNF-α level was induced 90 min after i.v. injection of LPS (1 μg/kg) in both groups (Fig. 1B). In biotin-deficient mice, the concentration of TNF-α was significantly ($P<0.05$) higher than that in biotin-sufficient mice. These results indicated that biotin deficiency augments TNF-α production in vivo.

In vitro effects of biotin deficiency on murine macrophages

Macrophages are the major cells that produce TNF-α in response to LPS. Therefore, we next examined the in vitro effects of biotin deficiency using J774.1 cells. In biotin-sufficient J774.1 cells, 130- and 80-kDa polypeptides were detected by Western blotting with HRP-conjugated avidin. On the other hand, these polypeptides were not detected after 2 weeks cultivation in biotin-deficient medium (**Fig. 2A**). On the basis of molecular weight, it is likely that the 130-kDa polypeptide is pyruvate carboxylase, and the 80-kDa polypeptide is propionyl-CoA carboxylase and/or methylcrotonyl-CoA carboxylase. Moreover, [^{3}H] TdR incorporation was significantly ($P<0.01$) lower in biotin-deficient cells than biotin-sufficient cells (Fig. 2B). These results clearly indicated that biotinylation of cellular proteins and cell proliferation was reduced by biotin deficiency.

Augmentation of LPS-induced TNF-α production in biotin-deficient J774.1 cells

Next, we analyzed the production of TNF-α from biotin-sufficient and -deficient J774.1 cells. As shown in **Figure 3A**, both types of cells produced TNF-α in response to LPS in a dose-dependent manner. The concentration of TNF-α in the culture supernatant of biotin-deficient cells was significantly ($P<0.01$) higher than that of biotin-sufficient cells, even without LPS stimulation. A similar pattern of TNF-α production was observed when the type of medium was replaced with the opposite type during LPS stimulation for 24 h, which excluded the possibility of contamination with stimulatory or inhibitory factors in either type of medium. LDH activity was not detected in the culture supernatant of biotin-deficient cells (data not shown), indicating that the augmentation of TNF-α production in biotin-deficient cells was not a result of plasma membrane damage. The levels of TNF-α mRNA were significantly ($P<0.01$) elevated in biotin-deficient cells compared with those in biotin-sufficient cells with or without LPS stimulation (Fig. 3B). Moreover, flow cytometric analysis revealed that the expression levels of cell surface and intracellular TNF-α were also higher in biotin-deficient cells than in biotin-sufficient cells (Fig. 3, C and D).

We also analyzed the effects of Act-D, an inhibitor of RNA polymerase II. In the presence of Act-D, intracellular TNF-α was decreased slightly in biotin-sufficient cells (**Fig. 4A**). On the other hand, it was markedly decreased in biotin-deficient cells (Fig. 4B) and in LPS-stimulated, biotin-sufficient cells (Fig. 4C). These results clearly indicated that biotin deficiency induces the augmentation of TNF-α production in vitro at the transcriptional level.

Cell surface expression of TNFRs

It was reported that biotin supplementation induces IL-2Rγ expression and decreases the net secretion of IL-2 by endocytosis of the cytokine [9]. Therefore, we measured cell surface expressions of TNFR types I and II on biotin-sufficient and -deficient J774.1 cells using a flow cytometer. As shown in **Figure 5, A** and **B**, the expression levels of TNF-R types I and II were similar between biotin-sufficient and -deficient cells. Mean fluorescence intensities of TNFR type I in biotin-sufficient and -deficient cells were 33.3 and 30.6, respectively; those of TNFR type II in biotin-sufficient and -deficient cells were 19.4 and 17.7, respectively. These results indicated that the augmentation of TNF-α production in biotin-deficient cells was not a result of down-regulation of the cell surface expression of TNFR and endocytosis of TNF-α.

Cell surface expression of CD14 and TLR4

To examine the possibility that biotin deficiency up-regulates LPS responsiveness through augmentation of LPS receptors, we measured the cell surface expression of CD14 and the TLR4/MD2 complex on biotin-sufficient and -deficient J774.1 cells.

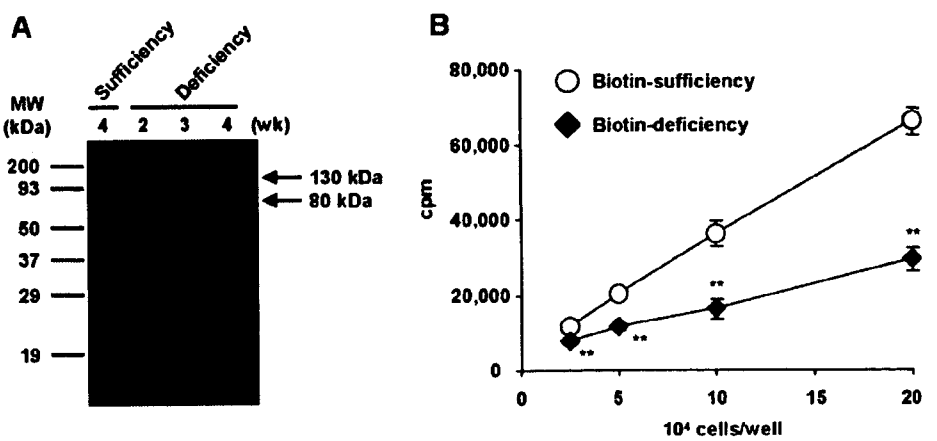

Fig. 2. In vitro effects of biotin deficiency on J774.1 cells, which were (A) cultured with biotin-sufficient or -deficient medium for the time indicated. Cells were lysed in SDS-PAGE sample buffer. Cell lysate (1×10^4 cells each) was subjected to Western blotting with HRP-conjugated avidin. (B) J774.1 cells were cultured with biotin-sufficient or -deficient medium for 4 weeks. Biotin-sufficient and -deficient cells in the medium with and without biotin, respectively, were seeded in 96-well flat-bottomed plates and incubated at 37°C for 3 h. Cells were pulsed with 1 kBq/well [^{3}H] TdR for 2 h. After the pulse, 100 μl 3% Triton X-100 was added to each well, and cells were harvested onto a glass fiber filter. **, $P<0.01$, compared with biotin sufficiency.

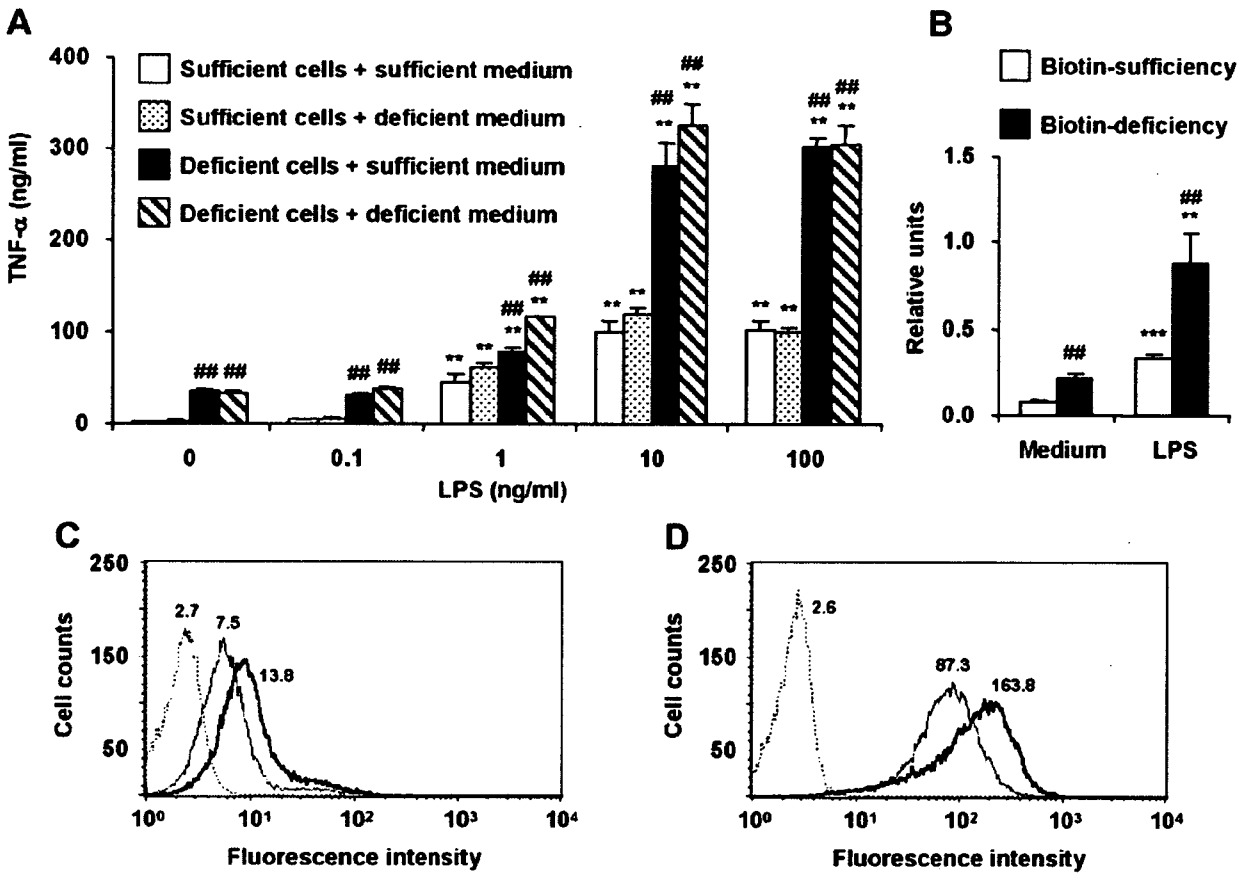

Fig. 3. TNF-α production of biotin-sufficient and -deficient J774.1 cells, which were cultured with biotin-sufficient or -deficient medium for 4 weeks. (A) Cells were seeded in 96-well flat-bottomed plates at 2×10^5 cells/200 μl/well with biotin-sufficient and -deficient medium and then stimulated with LPS at 37°C for 24 h. Concentrations of TNF-α in culture supernatants were measured by ELISA. **, $P < 0.01$, compared with medium alone (0 ng/ml LPS); ##, $P < 0.01$, compared with biotin sufficiency. (B) Biotin-sufficient and -deficient cells in medium with and without biotin, respectively, were seeded in 24-well flat-bottomed plates at 5×10^5 cells/500 μl/well and then stimulated with LPS (10 ng/ml) at 37°C for 4 h. TNF-α mRNA expression levels were determined by qRT-PCR. The results were expressed as relative units after normalization by the β-actin level. **, $P < 0.01$; ***, $P < 0.001$, compared with medium alone; ##, $P < 0.01$, compared with biotin sufficiency. (C and D) Cell surface (C) and intracellular TNF-α (D) of biotin-sufficient and -deficient cells were analyzed by flow cytometry. Dotted line, Unstained J774.1 cells (control); thin line, biotin sufficiency; bold line, biotin deficiency. Numbers in histograms indicate mean fluorescence intensity.

No differences were detected in the expression of these LPS receptors between biotin-sufficient and -deficient cells. Mean fluorescence intensities of CD14 in biotin-sufficient and -deficient cells were 9.0 and 9.2, respectively (Fig. 5C). Those of the TLR4/MD2 complex in biotin-sufficient and -deficient cells were 2.5 and 2.2, respectively (Fig. 5D). These results indicated that up-regulation of TNF-α production in biotin-deficient cells was not a result of augmentation of LPS receptors.

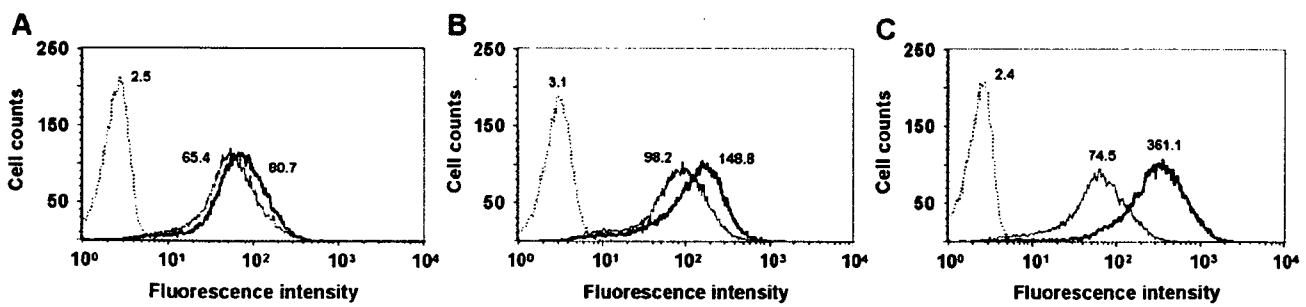

Fig. 4. Effects of Act-D on intracellular TNF-α levels of biotin-sufficient and -deficient J774.1 cells, which were cultured with biotin-sufficient or -deficient medium for 4 weeks. Biotin-sufficient and -deficient cells in the medium with and without biotin, respectively, were seeded in six-well flat-bottomed plates at 1×10^6 cells/2 ml/well with (thin line) or without (bold line) Act-D (1 μg/ml) at 37°C for 6 h. Intracellular TNF-α was analyzed by flow cytometry. The dotted line shows unstained J774.1 cells (control). (A) Biotin sufficiency without LPS; (B) biotin deficiency without LPS; (C) biotin sufficiency with LPS (10 ng/ml). Numbers in histograms indicate mean fluorescence intensity.

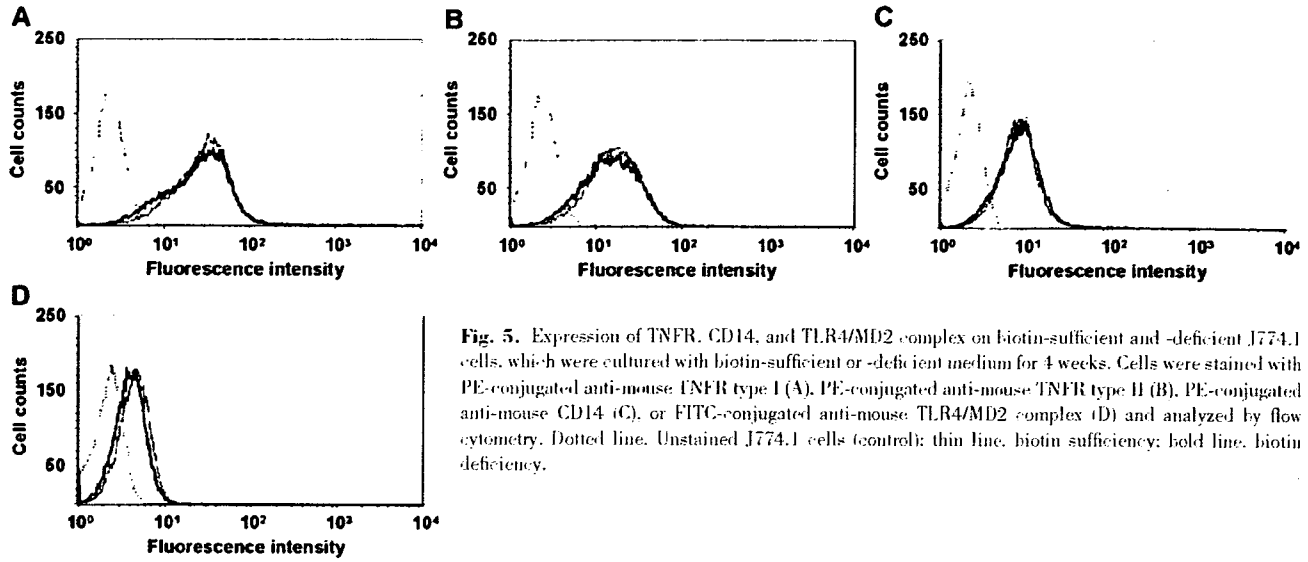

Fig. 5. Expression of TNFR, CD14, and TLR4/MD2 complex on biotin-sufficient and -deficient J774.1 cells, which were cultured with biotin-sufficient or -deficient medium for 4 weeks. Cells were stained with PE-conjugated anti-mouse TNFR type I (A), PE-conjugated anti-mouse TNFR type II (B), PE-conjugated anti-mouse CD14 (C), or FITC-conjugated anti-mouse TLR4/MD2 complex (D) and analyzed by flow cytometry. Dotted line, Unstained J774.1 cells (control); thin line, biotin sufficiency; bold line, biotin deficiency.

Activities of transcriptional factors in biotin-sufficient and -deficient J774.1 cells

We also analyzed the activities of two major transcriptional factors, which are responsible for TNF-α mRNA transcription—the NF-κB family (p65, p50, RelB, and p52) and AP-1 (phospho c-Jun)—in nuclear fractions of biotin-sufficient and -deficient J774.1 cells. The activities of NF-κB p65, p50, and AP-1 were increased significantly with LPS stimulation. However, no significant differences were detected in NF-κB family and AP-1 activities between biotin-sufficient and -deficient cells (**Fig. 6**), indicating that other factors are involved in the augmentation of TNF-α mRNA transcription in biotin-deficient cells.

Regulation of TNF-α levels by biotin supplementation in biotin-deficient J774.1 cells and biotin-deficient mice

To further confirm the effects of biotin deficiency, J774.1 cells were cultured with biotin-deficient medium for 4 weeks and then further incubated with biotin-sufficient medium for 2 weeks (biotin-supplement cells). [^{3}H] TdR incorporation in biotin-supplemented cells was still lower than that in biotin-

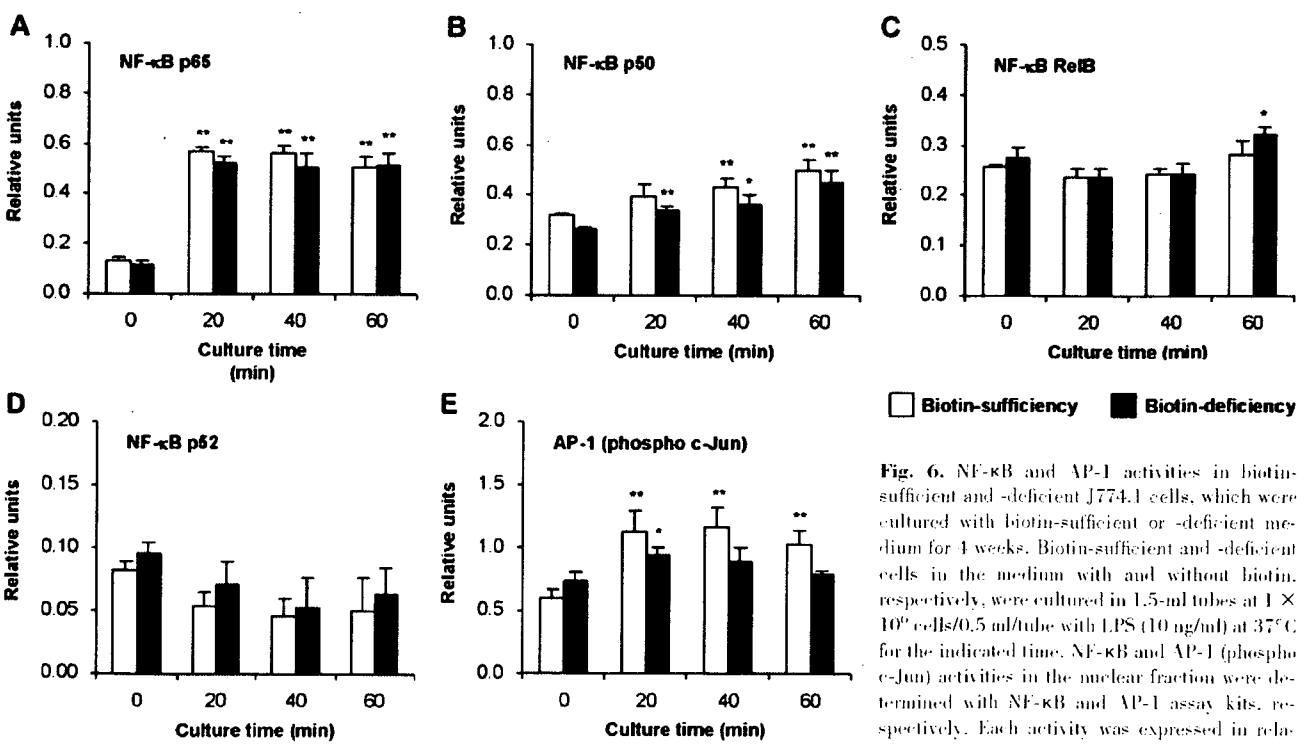

Fig. 6. NF-κB and AP-1 activities in biotin-sufficient and -deficient J774.1 cells, which were cultured with biotin-sufficient or -deficient medium for 4 weeks. Biotin-sufficient and -deficient cells in the medium with and without biotin, respectively, were cultured in 1.5-ml tubes at 1×10^6 cells/0.5 ml/tube with LPS (10 ng/ml) at 37°C for the indicated time. NF-κB and AP-1 (phospho c-Jun) activities in the nuclear fraction were determined with NF-κB and AP-1 assay kits, respectively. Each activity was expressed in relative units defined as $A_{450\ nm}$ per 100 μg protein. (A) NF-κB p65; (B) NF-κB p50; (C) RelB; (D) NF-κB p52; (E) AP-1. *, $P < 0.05$; **, $P < 0.01$, compared with no LPS stimulation (0 min).

sufficient cells but was significantly ($P<0.01$) higher than that in biotin-deficient cells (**Fig. 7A**). The concentrations of TNF-α in the culture supernatants of biotin-supplemented cells with and without LPS stimulation were significantly ($P<0.01$) reduced to near the levels in the supernatants of biotin-sufficient cells (Fig. 7B). The TNF-α production of biotin-deficient cells was significantly ($P<0.01$) decreased, even in the presence of 50 μM biotin during LPS stimulation (Fig. 7C). When biotin-deficient mice were provided with biotin-supplemented drinking water, the LPS-induced serum TNF-α levels of the mice were significantly ($P<0.05$) decreased (Fig. 7D). These results indicated that biotin supplementation restored the TNF-α production to the basal level in vitro and in vivo.

DISCUSSION

In this study, we clearly demonstrated that TNF-α production is up-regulated under biotin-deficient conditions and that biotin supplementation down-regulates the TNF-α production to the basal level in vivo and in vitro. These results suggest that biotin contributes to the regulation of inflammatory responses.

As biotin is produced by intestinal bacteria, many studies analyzed biotin-deficient animals that were fed a biotin-deficient diet containing egg-white protein, which contains avidin, a glycoprotein that forms a noncovalent and nonabsorbed complex with biotin [11–13, 23]. It was reported that biotin-deficient mice fed egg white for more than 7 weeks showed body weight loss and clinical symptoms, such as alopecia and

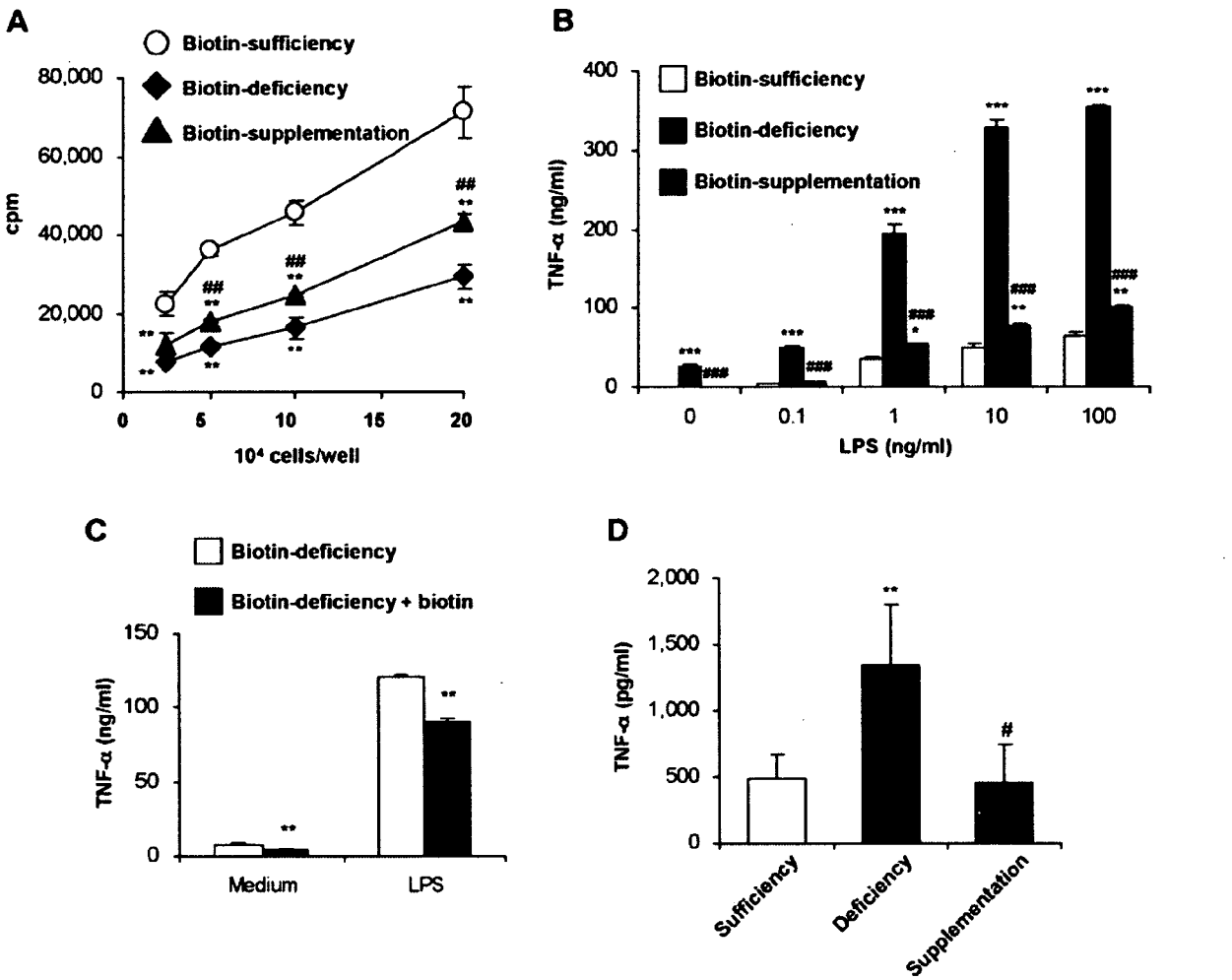

Fig. 7. Effects of biotin supplementation in vitro and in vivo. (A) J774.1 cells were cultured with biotin-deficient medium for 4 weeks and then incubated further in medium without biotin (biotin deficiency) or with biotin (biotin supplementation) for 2 weeks. J774.1 cells were also cultured in biotin-sufficient medium for 6 weeks (biotin sufficiency). [^{3}H] TdR incorporation is shown in Figure 2B. **, $P < 0.01$, compared with biotin sufficiency; ##, $P < 0.01$, compared with biotin deficiency. (B) Cells (2×10^5 cells/200 μl/well) in A were stimulated with LPS at 37°C for 24 h. Concentrations of TNF-α in culture supernatants were measured by ELISA. *, $P < 0.05$; **, $P < 0.01$; ***, $P < 0.001$, compared with biotin sufficiency; ###, $P < 0.001$, compared with biotin deficiency. (C) Cells (2×10^5 cells/200 μl/well) in A were stimulated with 10 ng/ml LPS in the presence of 50 μM biotin at 37°C for 24 h. Concentrations of TNF-α in culture supernatants were measured by ELISA. **, $P < 0.01$, compared with biotin deficiency (without biotin). (D) Mice were fed a biotin-deficient diet for 10 weeks (deficiency). Biotin-supplemented drinking water (15 μM) was administered to the mice for the last 2 weeks (biotin supplementation). The mice were then challenged i.v. with LPS (1 μg/kg) or saline alone, and blood was collected at 90 min after injection. Concentrations of TNF-α in sera were measured by ELISA. The results were expressed as mean ± SD for four mice. **, $P < 0.01$, compared with biotin sufficiency; #, $P < 0.05$, compared with biotin deficiency.

squatting posture [11]. Biotin-deficient rats fed egg white for 10 days showed partial alopecia and neurologic signs, such as kangaroo gait and irritability [13]. Moreover, severe biotin deficiency causes alopecia and scaly erythematous dermatitis in humans [11, 14, 15]. In this study, biotin-deficient mice were fed a biotin-deficient AIN-76 basal diet for 8 weeks, and the biotin concentrations in sera from biotin-deficient mice were significantly ($P<0.001$) lower than those from biotin-sufficient mice (Fig. 1A). However, PCC activities in the liver were comparable in biotin-sufficient and -deficient mice, and no body weight loss or clinical symptoms were detected. Therefore, we considered that our method causes mild biotin deficiency in mice.

Biotin-deficient J774.1 cells exhibited lower proliferation than biotin-sufficient cells (Fig. 2B). It was reported that intracellular uptake of biotin increases with cell proliferation [21]. As mentioned in Introduction, biotin-dependent carboxylases are essential for cellular metabolism, indicating that biotin deficiency causes inactivation of biotin-dependent carboxylases followed by the down-regulation of cellular metabolism and proliferation.

TNF-α production was augmented in biotin-deficient mice (Fig. 1B) and cells (Fig. 3). Biotin-deficient J774.1 cells produced a significantly higher amount of TNF-α, even without LPS stimulation. Moreover, the cell surface expression levels of the CD14 and TLR4/MD2 complex were not significantly different between biotin-sufficient and -deficient cells (Fig. 5, C and D). These results exclude the possibility that the augmentation of TNF-α production was mediated by up-regulation of LPS receptors. The TNF-α mRNA expression was significantly higher in biotin-deficient cells than -sufficient cells, and intracellular TNF-α was decreased markedly in the presence of Act-D (Fig. 4). It was reported that biotin supplementation up-regulates the expression level of the IL-2R and decreases the net production of IL-2 by endocytosis of cytokines [9]. However, no differences were detected in the expression levels of TNFR types I and II between biotin-sufficient and -deficient cells (Fig. 5, A and B). Furthermore, no differences were observed in the TNF-α-converting enzyme activities or mRNA levels of the tissue inhibitor of metalloproteinase-3, an inhibitor of the TNF-α-converting enzyme, between biotin-sufficient and -deficient cells (data not shown). The expression of intracellular and cell surface TNF-α was higher in biotin-deficient than -sufficient cells (Fig. 3, C and D). These results indicate that the augmentation of TNF-α production was regulated at the transcriptional level.

On the other hand, the biotin content in the AIN-76 diet (0.8 mg/kg) is much higher than the metabolic requirement of biotin. It was reported that the adequate intake of biotin for adult humans (~60 kg body weight) is 45 μg/day (0.75 μg/kg/day, Ministry of Health, Labor and Welfare, Japan). Based on the biotin content (0.8 mg/kg) and the total intake of diet (~5 g/day), biotin-sufficient mice (~25 g body weight) received 1 μg biotin per day (160 μg/kg/day). Moreover, the concentration of biotin in RPMI-1640 medium (0.2 μg/ml, ~800 nM) is much higher than biotin levels in normal mouse (40 nM) and human sera (0.2 nM) [11, 25]. Therefore, it is possible that the excess of biotin is involved in the down-regulation of TNF-α production.

No differences were detected in the activities of two major transcriptional factors involved in regulating TNF-α expression, namely NF-κB family members and AP-1 (Fig. 6). This result conflicts with the finding reported by Rodriguez-Melendez et al. [5] that the nuclear translocation and transcriptional activities of NF-κB were increased by biotin deficiency in Jurkat cells. The discrepancy may have been caused by the differences of cell line (murine macrophage cell line J774.1 and human T cell line Jurkat) or assay conditions. J774.1 cells were stimulated with LPS up to 60 min. On the other hand, Jurkat cells were stimulated with PMA and phytohemagglutinin for 3 h. Further studies are needed to clarify this point. It was reported that lysine residues in histones are modified by biotinylation, and the biotinylation of histones was enriched in transcriptionally inactive chromatin [6, 26, 27]. It is well known that some histone modifications, such as acetylation and methylation, correlate with transcriptional activation [28]. These observations suggest that the mechanism by which biotin deficiency contributes to up-regulation of TNF-α in J774.1 cells might be through biotin deficiency, producing reduced biotinylation of critical histones, leading to increased gene transcription.

Because of the uncertain immunological and pharmacological mechanisms, few studies have been reported about biotin treatment of inflammatory diseases [16]. On the other hand, it was reported that 10 nM biotin inhibited IL-2 production by Jurkat cells [8, 9]. Moreover, Zempleni et al. [10] reported that in vivo supplementation of biotin in healthy human subjects (3.1 μmol/day) inhibited IL-1β and IL-2 production of PBMCs. In this study, we demonstrated clearly that biotin supplementation down-regulated the augmented TNF-α production induced by biotin deficiency in vivo and in vitro (Fig. 7). Therefore, we speculate that a pharmacological dose of biotin might have some potentially therapeutic effects on inflammatory diseases, but this remains to be tested empirically.

TNF-α production of biotin-deficient J774.1 cells was drastically decreased by biotin supplementation in experiments in which biotin-deficient cells were cultured with biotin-sufficient medium (containing ~0.5 μM biotin) for 2 weeks (Fig. 7B). On the other hand, TNF-α production was similar in biotin-deficient cells cultured with biotin-sufficient and -deficient medium (Fig. 3A). A high dose of biotin (50 μM) slightly but significantly decreased TNF-α production by biotin-deficient cells (Fig. 7C). These results indicate that long-term supplementation of biotin is more effective for the inhibition of TNF-α up-regulation than stimulation with a high dose of biotin. Therefore, we considered that TNF-α up-regulation in biotin-deficient cells is regulated via various metabolic pathways that are affected by biotin rather than via the direct effects of biotin about TNF-α production.

It is well known that biotin deficiency causes cutaneous abnormalities [11, 14, 15]. In addition, it was reported that the biotin concentration in serum correlates with inflammatory diseases [11, 14, 15, 18]. Although several studies reported the contribution of abnormalities in lipid metabolism to cutaneous abnormalities (reviewed in ref. [11]), the pathological mechanisms of disease conditions caused by biotin deficiency remain to be clarified. In this study, we clearly demonstrated that biotin regulates TNF-α production in vivo and in vitro. TNF-α

plays important roles in the pathogenesis of inflammatory diseases, which have been reported to be correlated with biotin [29–31]. Therefore, biotin status may be involved in the pathological mechanisms of dermatitis and other inflammatory diseases. Our results should encourage further investigations on biotin treatment for various inflammatory diseases.

ACKNOWLEDGMENTS

This study was supported in part by Grants-in-Aid for Scientific Research from the Japan Society for the Promotion of Science (18791379) and a 21st Century Center for Excellence Program Special Research Grant from the Ministry of Education, Culture, Sports, Science, and Technology, Japan.

REFERENCES

1. Wood, H. G., Barden, R. E. (1977) Biotin enzymes. *Annu. Rev. Biochem.* **46**, 385–413.
2. Pacheco-Alvarez, D., Solórzano-Vargas, R. S., León-Del-Río, A. (2002) Biotin in metabolism and its relationship to human disease. *Arch. Med. Res.* **33**, 439–447.
3. Solórzano-Vargas, R. S., Pacheco-Alvarez, D., León-Del-Río, A. (2002) Holocarboxylase synthetase is an obligate participant in biotin-mediated regulation of its own expression and biotin-dependent carboxylases mRNA levels in human cells. *Proc. Natl. Acad. Sci. USA* **99**, 5325–5330.
4. Griffin, J. B., Rodriguez-Melendez, R., Zempleni, J. (2003) The nuclear abundance of transcription factors Sp1 and Sp3 depends on biotin in Jurkat cells. *J. Nutr.* **133**, 3409–3415.
5. Rodriguez-Melendez, R., Schwab, L. D., Zempleni, J. (2004) Jurkat cells respond to biotin deficiency with increased nuclear translocation of NF-κB, mediating cell survival. *Int. J. Vitam. Nutr. Res.* **74**, 209–216.
6. Stanley, J. S., Griffin, J. B., Zempleni, J. (2001) Biotinylation of histones in human cells. *Eur. J. Biochem.* **268**, 5424–5429.
7. De La Vega, L. A., Stockert, R. J. (2000) Regulation of the insulin and asialoglycoprotein receptors via cGMP-dependent protein kinase. *Am. J. Physiol. Cell Physiol.* **279**, C2037–C2042.
8. Manthey, K. C., Griffin, J. B., Zempleni, J. (2002) Biotin supply affects expression of biotin transporters, biotinylation of carboxylases and metabolism of interleukin-2 in Jurkat cells. *J. Nutr.* **132**, 887–892.
9. Rodriguez-Melendez, R., Camporeale, G., Griffin, J. B., Zempleni, J. (2003) Interleukin-2 receptor-γ-dependent endocytosis depends on biotin in Jurkat cells. *Am. J. Physiol. Cell Physiol.* **284**, C415–C421.
10. Zempleni, J., Helm, R. M., Mock, D. M. (2001) In vivo biotin supplementation at a pharmacologic dose decreases proliferation rates of human peripheral blood mononuclear cells and cytokine release. *J. Nutr.* **131**, 1479–1484.
11. Báez-Saldaña, A., Díaz, G., Espinoza, B., Ortega, E. (1993) Biotin deficiency induces changes in subpopulations of spleen lymphocytes in mice. *Am. J. Clin. Nutr.* **67**, 131–171.
12. Báez-Saldaña, A., Ortega, E. (2004) Biotin deficiency blocks thymocyte maturation, accelerates thymus involution, and decreases nose-rump length in mice. *J. Nutr.* **134**, 1970–1977.
13. Helm, R. M., Mock, N. L., Simpson, P., Mock, D. M. (2001) Certain immune markers are not good indicators of mild to moderate biotin deficiency in rats. *J. Nutr.* **131**, 3231–3236.
14. Mock, D. M. (1994) Skin manifestations of biotin deficiency. *Semin. Dermatol.* **10**, 290–302.
15. Proud, V. K., Rizzo, W. B., Patterson, J. W., Heard, G. S., Wolf, B. (1990) Fatty-acid alterations and carboxylase deficiencies in the skin of biotin-deficient rats. *Am. J. Clin. Nutr.* **51**, 853–858.
16. Machashi, M., Makino, Y., Furukawa, Y., Ohinata, K., Kimura, S., Satoh, T. (1993) Effect of biotin treatment on metabolic abnormalities occurring in patients with stenocostoclavicular hyperostosis. *J. Clin. Biochem. Nutr.* **15**, 65–76.
17. Nakamura, K., Imakado, S., Takizawa, M., Adachi, M., Sugaya, M., Wakugawa, M., Asahina, A., Tamaki, K. (2000) Exacerbation of pustulosis palmaris et plantaris after topical application of metals accompanied by elevated levels of leukotriene B_4 in pustules. *J. Am. Acad. Dermatol.* **42**, 1021–1025.
18. Makino, Y., Osada, K., Sone, H., Sugiyama, K., Konai, M., Ito, M., Tsunoda, K., Furukawa, Y. (1999) Percutaneous absorption of biotin in healthy subjects and in atopic dermatitis patients. *J. Nutr. Sci. Vitaminol. (Tokyo)* **45**, 347–352.
19. Baumgartner, E. R., Suormala, T. (1997) Multiple carboxylase deficiency: inherited and acquired disorders of biotin metabolism. *Int. J. Vitam. Nutr. Res.* **67**, 377–384.
20. Koyama, R., Imaizumi, K., Suzuki, K., Tanaka, T. (1969) *Practical Guide on the Laboratory Animal Care*, Tokyo, Japan, Igaku Shoin.
21. Mock, D. M. (1997) Determination of biotin in biological fluids. *Methods Enzymol.* **279**, 265–275.
22. Zempleni, J., Timothy, A., Mock, D. M. (1997) Lipoic acid reduces the activity of biotin-dependent carboxylases in rat liver. *J. Nutr.* **127**, 1776–1781.
23. Rabin, B. S. (1983) Inhibition of experimentally induced autoimmunity in rats by biotin deficiency. *J. Nutr.* **113**, 2316–2322.
24. Zempleni, J., Mock, D. M. (1999) Mitogen-induced proliferation increases biotin uptake into human peripheral blood mononuclear cells. *Am. J. Physiol.* **276**, C1079–C1084.
25. Mock, D. M., Lankford, G. L., Mock, N. I. (1995) Biotin accounts for only half of the total avidin-binding substances in human serum. *J. Nutr.* **125**, 941–946.
26. Hassan, Y. I., Zempleni, J. (2006) Epigenetic regulation of chromatin structure and gene function by biotin. *J. Nutr.* **136**, 1763–1765.
27. Peters, D. M., Griffin, J. B., Stanley, J. S., Beck, M. M., Zempleni, J. (2002) Exposure to UV light causes increased biotinylation of histones in Jurkat cells. *Am. J. Physiol. Cell Physiol.* **283**, C878–C884.
28. Strahl, B. D., Allis, C. D. (2000) The language of covalent histone modifications. *Nature* **403**, 41–45.
29. Villagomez, M. T., Bae, S-J., Ogawa, L., Takenaka, M., Katayama, I. (2004) Tumor necrosis factor-α but not interferon-γ is the main inducer of inducible protein-10 in skin fibroblasts from patients with atopic dermatitis. *Br. J. Dermatol.* **150**, 910–916.
30. Nakae, S., Komiyama, Y., Narumi, S., Sudo, K., Horai, R., Tagawa, Y., Sekikawa, K., Matsushima, K., Asano, M., Iwakura, Y. (2003) IL-1-induced tumor necrosis factor-α elicits inflammatory cell infiltration in the skin by inducing IFN-γ-inducible protein 10 in the elicitation phase of the contact hypersensitivity response. *Int. Immunol.* **15**, 251–260.
31. Murakata, H., Harabuchi, Y., Kataura, A. (1999) Increased interleukin-6, interferon-γ and tumor necrosis factor-α production by tonsillar mononuclear cells stimulated with α-streptococci in patients with pustulosis palmaris et plantaris. *Acta Otolaryngol.* **119**, 384–391.

Blockade of NKG2D on NKT cells prevents hepatitis and the acute immune response to hepatitis B virus

Sílvia Vilarinho*†, Kouetsu Ogasawara‡§, Stephen Nishimura¶, Lewis L. Lanier†§, and Jody L. Baron*†‖

*Department of Medicine, †Liver Center, §Department of Microbiology and Immunology and the Cancer Research Institute, and ¶Department of Pathology, University of California, San Francisco, CA 94143

Communicated by Arthur Weiss, University of California School of Medicine, San Francisco, CA, September 20, 2007 (received for review July 12, 2007)

Hepatitis B virus (HBV) is a hepadnavirus that is a major cause of acute and chronic hepatitis in humans. Hepatitis B viral infection itself is noncytopathic, and it is the immune response to the viral antigens that is thought to be responsible for hepatic pathology. Previously, we developed a transgenic mouse model of primary HBV infection and demonstrated that the acute liver injury is mediated by nonclassical natural killer (NK)T cells, which are CD1d-restricted, but nonreactive to α-GalCer. We now demonstrate a role for NKG2D and its ligands in this nonclassical NKT cell-mediated immune response to hepatitis B virus and in the subsequent acute hepatitis that ensues. Surface expression of NKG2D and one of its ligands (retinoic acid early inducible-1 or RAE-1) are modulated in an HBV-dependent manner. Furthermore, blockade of an NKG2D–ligand interaction completely prevents the HBV- and CD1d-dependent, nonclassical NKT cell-mediated acute hepatitis and liver injury. This study has major implications for understanding activation of NKT cells and identifies a potential therapeutic target in treating hepatitis B viral infection.

Infection with hepatitis B virus (HBV) is a major cause of liver disease worldwide. More than 350 million people are persistently infected with HBV (1, 2). Hepatitis B viral infection itself is noncytopathic, and it is the immune response to the viral antigens that is thought to be responsible for the necroinflammatory process involved in chronic infection, cirrhosis, and hepatocellular carcinoma (3, 4). Thus, understanding the pathogenesis of acute and chronic HBV infection mandates understanding the immune responses underlying these processes. Unfortunately, the study of HBV immunopathogenesis has been problematic because natural hepadnaviral infections occur only in outbred species whose immune systems are difficult to experimentally manipulate.

We have established a transgenic mouse model of primary HBV infection that allows the study of mechanisms underlying the immunopathogenesis of hepatitis B virus-induced disease. To generate this mouse model of primary HBV infection, we used either mice that express the small, middle, and large envelope proteins of HBV as transgenes in the liver by using an albumin promoter (hereafter designated HBV-Env$^+$) (5) or mice that express a terminally redundant HBV DNA construct as a transgene and display intrahepatic HBV replication (hereafter designated HBV-Replication$^+$) (6). We ablated the resident adaptive immune system of these HBV-transgenic mice, in which the B and T cells are tolerant to HBV, by crossing the HBV-transgenic mice to mice with mutations in the recombinase activating genes (*RAG-1*) (7). We then reconstituted the immune system in these mice by the adoptive transfer of unimmunized splenocytes isolated from syngeneic, wild-type mice. In this way, a liver with HBV-expressing hepatocytes is exposed to a healthy, untolerized, naïve immune system, just as in acute HBV infection of humans. This system results in a biphasic illness, with a rapid acute hepatitis, followed by a smoldering chronic hepatitis (8).

In this model of HBV infection, a spontaneous, natural immune response to hepatitis B virus is generated. Because this experimental system mimics primary HBV infection, we can uniquely study innate and adaptive immune responses to HBV. Our previous results using this model demonstrated that natural killer (NK)T cells (and not NK cells or conventional αβ-TcR T cells) alone are sufficient to induce hepatitis when adoptively transferred into HBV transgenic RAG$^{-/-}$ mice. Furthermore, we demonstrated, using several different experimental approaches, that this population of NKT cells that mediates acute hepatitis is nonclassical in that these cells do not recognize the classic NKT cell ligand, α-galactosylceramide CD1d and do not express the canonical T cell receptor Vα14; but activation of these cells depends on expression of CD1d and HBV.

Innate immune effector cells mediate the acute hepatitis in our model, although the mechanism of activation of these cells in response to the presence of HBV in liver is unclear. Our previous data suggest that the presence of HBV leads to alterations in the class I-like molecule CD1d and, subsequently, to the activation of nonclassical NKT cells and hepatitis (8). NKT and NK cells share many of the same activating and inhibitory receptors. One of the activating receptors is NKG2D, a type II transmembrane-anchored glycoprotein, which has been shown to be an activating or costimulatory receptor expressed on the surface of all NK cells, activated CD8$^+$ T lymphocytes, and most γ/δ T cells, both in mice and humans (9–11). Although NKG2D is known to also be expressed on the surface of NKT cells (12, 13), a role for NKG2D in NKT cell activation has never been demonstrated.

NKG2D binds to a family of ligands with structural homology to MHC class I molecules. In contrast to classical MHC molecules, NKG2D ligands do not require association with β_2 microglobulin for expression or function, and do not bind antigenic peptides (14). In mice, NKG2D ligands include the retinoic acid early-inducible 1 family of proteins (RAE-1α, β, γ, δ, ε), H60, and MULT1 (15–17). The ligands of NKG2D are known to be "stress-inducible" molecules, whose expression is triggered by cellular transformation, viral infection (9), and/or DNA damage (18).

In this study, we addressed the question of whether NKG2D and its ligands play a role in the nonclassical NKT cell-mediated immune response to HBV and the subsequent acute hepatitis that ensues. Our results demonstrate that NKG2D is modulated on NK and NKT cells at the time of acute hepatitis; and the presence of HBV in the livers of our transgenic mice can lead to an increase in RAE-1 surface expression on hepatocytes. Furthermore, blockade

Author contributions: S.V., L.L.L., and J.L.B. designed research; S.V. and S.N. performed research; K.O. and L.L.L contributed new reagents/analytic tools; S.V., S.N., L.L.L., and J.L.B. analyzed data; and S.V. and J.L.B. wrote the paper.

Conflict of interest statement: The authors declare a conflict of interest (such as defined by PNAS policy). University of California (San Francisco, CA) has licensed intellectual property rights relating to this research for potential therapeutic development.

Abbreviations: ALT, alanine aminotransferase; HBV, hepatitis B virus; NK, natural killer; RAE-1, retinoic acid early-inducible-1; MULT1, murine ULBP-like transcript 1; RAG$^{-/-}$, recombinase activating gene-1.

‡Present address: Department of Intractable Diseases, Division of Clinical Immunology, Research Institute, International Medical Center of Japan, 1-21-1 Toyama, Shinjuku-ku, Tokyo 162-8655, Japan.

‖To whom correspondence should be addressed at: Department of Medicine, GI Division, University of California, 513 Parnassus Avenue, Room S357C, Box 0538, San Francisco, CA 94143-0538. E-mail: jody.baron@ucsf.edu.

This article contains supporting information online at www.pnas.org/cgi/content/full/0708968104/DC1.

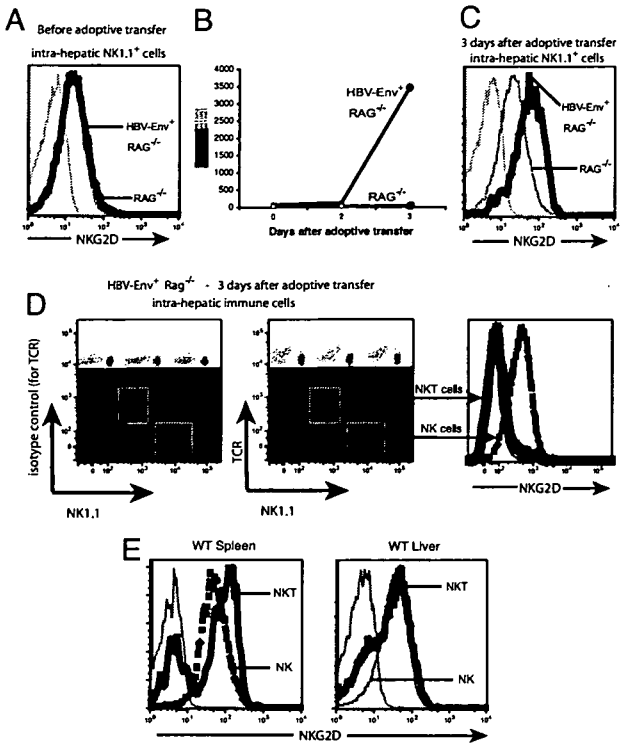

Fig. 1. Modulation of the NKG2D receptor during acute hepatitis. (*A* and *C*) NKG2D expression on the surface of NK1.1$^+$ cells from HBV-Env$^+$ RAG$^{-/-}$ (heavy black line) and RAG$^{-/-}$ (dotted line) before (*A*) and 3 days after (*C*) adoptive transfer of 10^8 splenocytes. (*B*) Hepatic necrosis in these animals was assessed by the measurement of ALT in the sera of RAG$^{-/-}$ (○) or HBV-Env$^+$ RAG$^{-/-}$ (●) mice. ALT values are shown as mean ± SEM. (*D*) Surface expression of NKG2D on intrahepatic NKT (heavy black line) and NK cells (dashed line) from HBV-Env$^+$ RAG$^{-/-}$ mice 3 days after adoptive transfer. The left dot plot depicts the isotype-matched control Ig staining of TCR on NKT cells. (*E*) Surface expression of NKG2D on NKT cells (heavy black line) and NK cells (dashed line) from the spleen and liver of wild-type mice. The shaded histograms depict staining using an isotype-matched control rat IgG1. All experiments were repeated at least three times, and representative data are shown.

of an NKG2D–ligand interaction completely prevents the HBV-specific and CD1d-dependent, nonclassical NKT cell-mediated acute hepatitis and liver injury.

Results

NKG2D Expression Is Modulated on Intrahepatic Immune Cells from HBV-Env$^+$ RAG$^{-/-}$ Mice with Acute Hepatitis. Our previous studies have demonstrated that activation of nonclassical NKT cells is necessary for the acute hepatitis to develop and that NK cells or conventional T cells alone cannot initiate the acute hepatitis (8). NK1.1$^+$ cells from the livers of HBV-Env$^+$ RAG$^{-/-}$ and RAG$^{-/-}$ mice before adoptive transfer of syngeneic naïve splenocytes expressed equivalent amounts of NKG2D on their surface (Fig. 1*A*). However, when we analyzed the expression of NKG2D on liver lymphoid cells during the acute immune response and hepatitis seen in the livers of HBV-expressing mice with reconstituted immunity (Fig. 1*B*), we found that NK1.1$^+$ cells from HBV-Env$^+$ RAG$^{-/-}$ mice (which include both resident and donor NK cells and donor NKT cells) expressed higher levels of NKG2D than the same population eluted from RAG$^{-/-}$ mice that also had reconstituted immunity (Fig. 1*C*).

We next analyzed the surface expression of NKG2D on the NKT and NK populations in the liver at the peak of acute hepatitis. We found that NK cells eluted from the livers of HBV-Env$^+$ RAG$^{-/-}$ mice with acute hepatitis expressed high levels of NKG2D (Fig. 1*D*), but the majority of activated NKT cells expressed very low levels of NKG2D on their cell surface (Fig. 1*D*). Because the majority of NKT cells in the spleen (the cells adoptively transferred) and liver of wild-type mice expressed high levels of NKG2D (Fig. 1*E*), this result suggests that NKT cells eluted from the livers of the HBV-Env$^+$ RAG$^{-/-}$ mice have down-regulated the surface expression of NKG2D. This is consistent with the fact that NKG2D is known to be internalized after interaction with its ligands (8, 14, 19). Taken together, these results suggest that NKG2D expression is up-regulated on the NK cells, and down-regulated on the NKT cells, during acute hepatitis.

Constitutive Surface Expression of RAE-1 on Hepatocytes Is Elevated Specifically on HBV-Env$^+$ Hepatocytes. In light of these data, we examined the expression of NKG2D ligands on wild-type nontransgenic hepatocytes and on HBV-Env$^+$ hepatocytes. In the genetic background of the HBV-transgenic mice (B10.D2 and C57BL/6), the NKG2D ligands expressed are *RAE-1δ*, *RAE-1ε*, and MULT1 (14). Although RAE-1 is not expressed in most tissues isolated from healthy, adult mice, RAE-1 is transcribed preferentially in liver of healthy, adult mice (http://source.stanford.edu/cgi-bin/source/sourceSearch). We examined the expression of these NKG2D ligand proteins on primary hepatocytes and intrahepatic immune cells of HBV-Env$^+$ RAG$^{-/-}$ and wild-type nontransgenic RAG$^{-/-}$ mice before adoptive transfer. We found constitutive low-level surface expression of RAE-1 on hepatocytes from RAG$^{-/-}$ mice, which was increased specifically on the surface of HBV-Env$^+$ hepatocytes (Fig. 2*A*). This constitutive expression of RAE-1 on hepatocytes, and increased expression in the HBV-Env$^+$ transgenic mice, was also found in wild-type mice that were not crossed to RAG$^{-/-}$ mice (data not shown). We found no expression of RAE-1 on splenocytes or on intrahepatic immune cells from HBV-Env$^+$ RAG$^{-/-}$ mice, RAG$^{-/-}$ mice, or wild-type mice (Fig. 2*B* and data not shown). The constitutive surface expression of RAE-1 on hepatocytes is an interesting finding, because the expression of RAE-1 family members is strictly regulated in normal cells, and little expression is found on healthy adult tissue (14). Increased RAE-1 expression on hepatocytes from HBV-Env$^+$ RAG$^{-/-}$ mice demonstrates that RAE-1 can be modulated on hepatocytes in an HBV-specific manner. We did not detect MULT1 expression, or a change in either MHC class I or CD1d expression, on primary hepatocytes derived from either HBV-Env$^+$ RAG$^{-/-}$ or RAG$^{-/-}$ mice or on intrahepatic immune cells (data not shown).

Constitutive expression of RAE-1 on primary hepatocytes from RAG$^{-/-}$ mice was confirmed by quantitative PCR of reverse-transcribed RAE-1 mRNA normalized to the expression of *Hprt* transcripts (Fig. 2*B*). Increased RAE-1 expression on hepatocytes from HBV-Env$^+$ RAG$^{-/-}$ mice, as compared with RAG$^{-/-}$ mice, was also confirmed by quantitative RT-PCR. There was an almost 7-fold increase in RAE-1 mRNA from HBV-Env$^+$ RAG$^{-/-}$ hepatocytes, as compared with RAG$^{-/-}$ hepatocytes (Fig. 2*B*).

Blocking of an NKG2D–Ligand Interaction *in Vivo* Prevents the Acute Immune Response to Human HBV. In view of the fact that NKG2D and one of its ligands are modulated during the acute immune response to HBV, we studied the effects of blocking this interaction on the onset of the acute hepatitis by using an anti-mouse NKG2D monoclonal antibody (CX5), which efficiently blocks the binding of NKG2D to its ligands and does not deplete NKG2D-bearing cells *in vivo* (20). HBV-Env$^+$ RAG$^{-/-}$ recipient mice were treated with 200 μg of anti-NKG2D mAb (CX5) or control rat IgG the day before and 4 days after adoptive transfer of syngeneic naïve splenocytes. Blocking the NKG2D receptor completely prevented acute liver injury in all HBV-Env$^+$ RAG$^{-/-}$ mice, whereas the control antibody had no effect as all mice showed signs of massive acute hepatitis, as revealed by the elevated serum ALT values at days 3 and 4 after adoptive transfer (Fig. 3*A*). Histological analyses

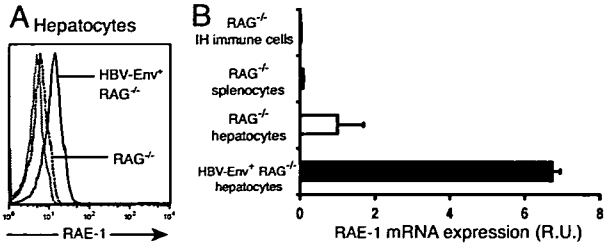

Fig. 2. Constitutive surface expression of the NKG2D ligand RAE-1 on hepatocytes is up-regulated specifically on HBV-Env-expressing hepatocytes, before adoptive transfer. (*A*) Surface expression of RAE-1 on hepatocytes from HBV-Env$^+$ RAG$^{-/-}$ (solid line) and RAG$^{-/-}$ (dotted line) mice. Shaded histograms depict staining using the appropriate isotype-matched control Ig. (*B*) RAE-1 mRNA expression in hepatocytes from HBV-Env$^+$ RAG$^{-/-}$ (black bar) and RAG$^{-/-}$ (white bar) mice and from intrahepatic (IH) immune cells and splenocytes from RAG$^{-/-}$ mice in comparison with HPRT expression. All data are representative of at least three independent experiments.

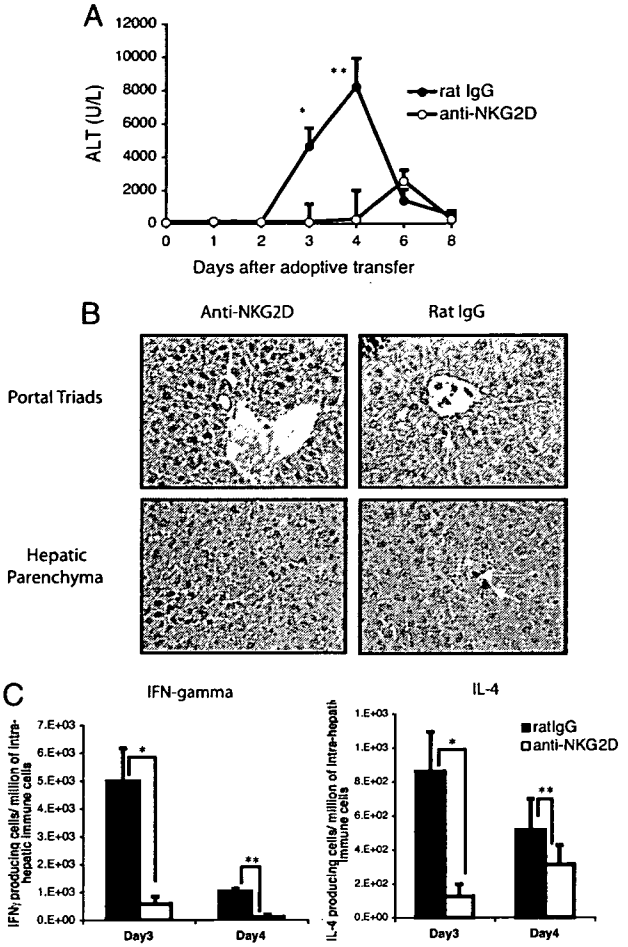

Fig. 3. Blocking NKG2D *in vivo* prevents the liver injury caused by the acute immune response to HBV. (*A*) Serum ALT levels of HBV-Env$^+$ RAG$^{-/-}$ mice treated with anti-NKG2D mAb (○) or rat IgG (●). The ALT values as mean ± SEM are shown. Student's *t* test analyses: *, $P < 0.02$; **, $P < 0.01$. (*B*) Hematoxylin and eosin-stained section (magnification ×20) of portal triads (*Upper*) and hepatic lobular parenchyma (*Lower*) from HBV-Env$^+$ RAG$^{-/-}$ mice treated with anti-NKG2D mAb (*Left*) or rat IgG (*Right*), 4 days after the adoptive transfer of 10^8 splenocytes. Arrows point to necrotic hepatocytes, and asterisks indicate inflammatory infiltrate. (*C*) Elispot analyses of IFN-γ- and IL4-producing intrahepatic immune cells from HBV-Env$^+$ RAG$^{-/-}$ mice treated with control rat IgG (black bars) or anti-NKG2D mAb (white bars) at days 3 and 4 after adoptive transfer. Representative data are shown as mean ± SD. Student's *t* test analyses: *, $P < 0.005$; **, $P < 0.02$. All data are representative of at least three independent experiments.

of liver sections also showed that mice treated with control IgG developed a severe hepatitis, pathologically characterized by parenchymal inflammation, hepatocellular damage, and portal inflammation and necrotic hepatocytes at day 4 after adoptive transfer (Fig. 3*B*). These histological abnormalities were absent at the same time point in all mice treated with anti-NKG2D mAb (Fig. 3*B*). These results demonstrate a fundamental role played by NKG2D in the acute immune response to HBV-expressing hepatocytes, and the consequent development of hepatitis and hepatic necrosis.

HBV-Env$^+$ RAG$^{-/-}$ mice have an HBV-dependent increase in the frequency of IFN-γ- and IL-4-producing cells in their livers 3 days after adoptive transfer (8). Because NKT cells mediate this cytokine burst detected at the time of acute hepatitis, we investigated the cytokine profile of lymphoid cells in anti-NKG2D or control IgG-treated HBV-Env$^+$ RAG$^{-/-}$ mice. We quantified the number of IFN-γ- and IL-4-producing intrahepatic immune cells by Elispot at days 3 and 4 after adoptive transfer of syngeneic wild-type splenocytes. Three days after the adoptive transfer, the number of IFN-γ- and IL-4-producing cells increased by 8- and 7-fold, respectively, in mice that received control IgG (and developed hepatitis) as compared with NKG2D-blocked mice (Fig. 3*C*). A similar difference was observed on day 4 after adoptive transfer. These data demonstrate that blocking of NKG2D also severely impaired the production of cytokines by intrahepatic immune cells in mice expressing HBV antigens. Flow cytometric analysis of the intrahepatic immune cells derived from the anti-NKG2D or control IgG-treated HBV-Env$^+$ RAG$^{-/-}$ mice revealed that the absolute number of NK cells eluted from both groups of mice was similar, whereas the absolute number of NKT cells was reduced by 2- and 3-fold in the mice that received the anti-NKG2D treatment and did not develop hepatitis [supporting information (SI) Table 1]. This specific reduction in the number of NKT cells, but not NK cells, in the livers of the anti-NKG2D-treated mice suggests that the antibody is specifically affecting the NKT cells.

NKG2D Receptor Expression on NKT Cells Is Required for Efficient Disease Induction. NKG2D is expressed on ≈60% of NKT cells in the spleen (Fig. 1*E*). To determine whether donor NKT cells expressing NKG2D are responsible for induction of the acute hepatitis after transfer into HBV-Env$^+$ RAG$^{-/-}$ mice, splenocytes from wild-type mice were depleted of NKG2D$^+$ lymphocytes by flow cytometric cell sorting. NKG2D-depleted splenocytes were adoptively transferred into HBV-Env$^+$ RAG$^{-/-}$ recipients. In this way, the transferred donor NKT cells would not express surface NKG2D, but resident NK cells in the recipient mice would still express NKG2D. HBV-Env$^+$ RAG$^{-/-}$ mice received NKG2D-depleted splenocytes or appropriate controls for the total number of splenocytes, or total number of NK and NKT cells transferred. The HBV-Env$^+$ RAG$^{-/-}$ recipient mice received one of three different populations of donor splenocytes: 50 million NKG2D-depleted splenocytes (which included 1.25×10^5 NKG2D$^-$ NKT cells, and no NK cells); 50 million unsorted splenocytes (which included 2.5×10^5 unsorted NKT cells and 1.25×10^6 NK cells); or 33 million NK cell-depleted splenocytes (which included 1.25×10^5 unsorted NKT cells, and no NK cells). In this latter group, the NK cells were depleted from the donor mice by injection of anti-asialoGM1 antisera, which is known to deplete NK cells, but not NKT cells (21).

The depletion of NKG2D$^+$ NKT cells, but not the depletion of NKG2D-bearing NK cells, from donor splenocytes significantly diminished the acute liver injury and cytokine burst seen in the

IMMUNOLOGY

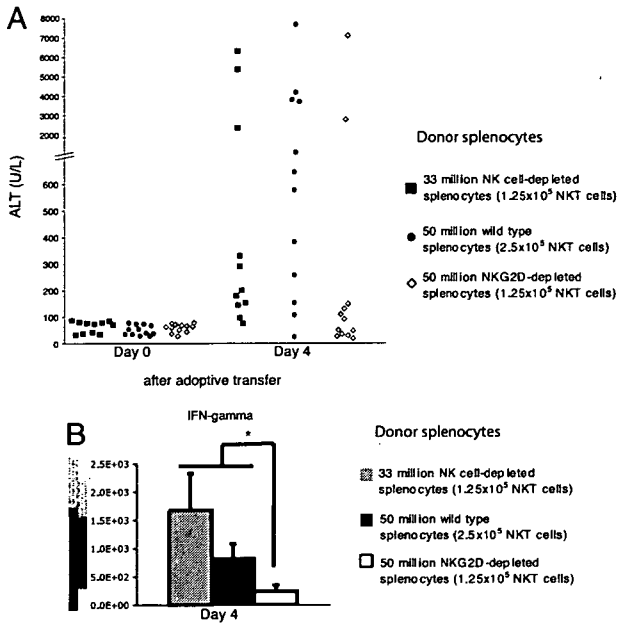

Fig. 4. NKG2D$^+$ NKT cells are required for efficient disease induction and cytokine production during the acute immune response to HBV. (*A*) Hepatic injury of HBV-Env$^+$ RAG$^{-/-}$ mice at day 4 after adoptive transfer of 50 × 10^6 NKG2D-depleted splenocytes (which included 1.25 × 10^5 NKG2D$^-$ NKT cells, and no NK cells) (open diamonds) was compared with hepatic injury in HBV-Env$^+$ RAG$^{-/-}$ mice that received the same total number of unsorted wild-type splenocytes (50 × 10^6, which included 2.5 × 10^5 unsorted NKT cells, and 1.25 × 10^6 NK) (filled circles) (Mann–Whitney test analyses: $P < 0.02$) or that received the same total number of unsorted NKT cells and NK cells (33 × 10^6, which included 1.25 × 10^5 unsorted NKT cells, and no NK cells) (filled squares). (Mann–Whitney test analyses: $P < 0.03$). (*B*) Elispot analyses of IFN-γ producing intrahepatic immune cells from HBV-Env$^+$ RAG$^{-/-}$ mice depicted in *A*. Representative data are shown as mean ± SD. Student's *t* test analyses: *, $P < 0.001$.

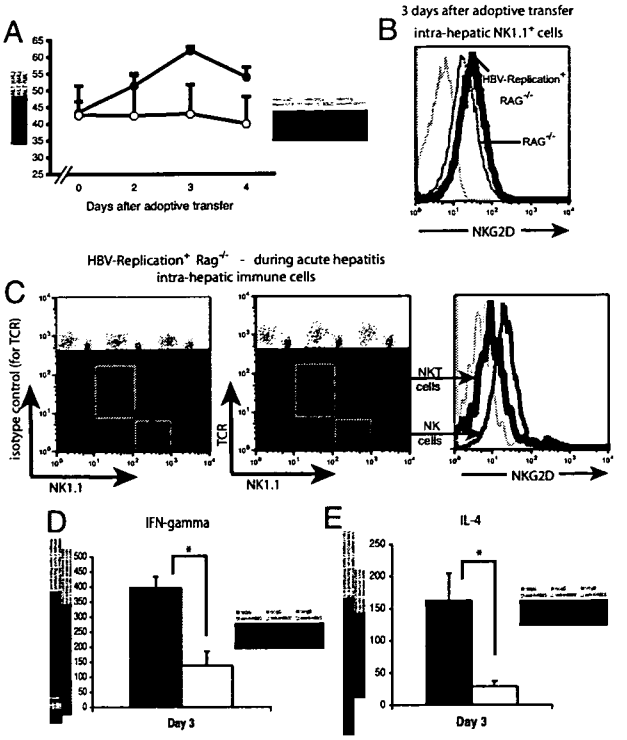

Fig. 5. Blocking an NKG2D–ligand interaction in HBV-Replication$^+$ RAG$^{-/-}$ mice prevents liver injury and cytokine production mediated by the acute immune response to HBV. (*A*) Serum ALT levels of HBV-Replication$^+$ RAG$^{-/-}$ mice treated with anti-NKG2D mAb (○) or rat IgG (●) at 2, 3, and 4 days after adoptive transfer of 1 × 10^8 syngeneic splenocytes are shown as mean ± SEM. (*B*) NKG2D surface expression on intrahepatic NK1.1$^+$ cells from HBV-Replication$^+$ RAG$^{-/-}$ mice (heavy black line) as compared with RAG$^{-/-}$ mice (dotted line) at day 3 after the adoptive transfer of syngeneic naïve splenocytes. Shaded histogram depicts staining using the appropriate isotype-matched control Ig (rat IgG1). (*C*) Surface expression of NKG2D on intrahepatic NKT (heavy black line) and NK cells (lighter black line) from HBV-Replication$^+$ RAG$^{-/-}$ mice 3 days after adoptive transfer. The left dot plot depicts the isotype-matched control Ig staining of TCR on NKT cells. (*D* and *E*) Elispot analyses of IFN-γ (*D*) and IL-4-producing (*E*) intrahepatic immune cells from HBV-Replication$^+$ RAG$^{-/-}$ mice treated with rat IgG (black bars) or anti-NKG2D mAb (white bars) at day 3 after adoptive transfer. Representative data are shown as mean ± SD. Student's *t* test analyses: *, $P < 0.001$. All data are representative of at least two independent experiments.

HBV-Env$^+$ RAG$^{-/-}$ mice as compared with either control group (Fig. 4 *A* and *B*). Thus, NKG2D receptor expression on NKT cells and not on NK cells is required for efficient disease induction. The finding that depletion of NKG2D-bearing cells did not completely eliminate all disease in all recipient mice could be accounted for the fact that the NKG2D$^-$ NKT cells to begin to express surface NKG2D after adoptive transfer (data not shown). Further evidence that NKG2D expression only on NKT cells is necessary for disease induction comes from the finding that depletion of NKG2D$^+$ NKT cells from donor splenocytes completely prevented induction of acute hepatitis in the HBV-Env$^+$ RAG$^{-/-}$ mice (SI Fig. 6). Thus, NKG2D expression on NKT cells, and not on any other cell types, is necessary for induction of hepatitis.

NKG2D Blockade Prevents Acute Hepatitis and the Cytokine Burst Seen in HBV-Replication$^+$ RAG$^{-/-}$ Transgenic Mice. To assess the relevance of our observations to responses to authentic human HBV infection, we characterized the role of NKG2D in the acute immune response developed in HBV-Replication$^+$ RAG$^{-/-}$ mice, which display intrahepatic HBV replication and produce infectious virions (6). Reminiscent of the usual initial presentation of human HBV infection, these mice develop a mild, subclinical hepatitis after adoptive transfer of naïve splenocytes. Analogous to our observations in the HBV-Env$^+$ RAG$^{-/-}$ mice, this hepatitis is mediated by nonclassical NKT cells in an HBV-specific and CD1d-dependent manner, leading to cytokine production (ref. 8 and unpublished data). Although the severity of hepatitis seen in the two lines of HBV-transgenic mice is different, owing to an increase in hepatocyte sensitivity to cytotoxic effects of IFN-γ in the HBV-Env$^+$ mice (22), a similar disease pattern is seen in both lines of HBV-transgenic mice. Specifically, a biphasic ALT rise that is seen in the HBV-Env$^+$ RAG$^{-/-}$ mice is also observed in the HBV-Replication$^+$ RAG$^{-/-}$ mice, but, as expected, the ALT rise is much more modest than that seen in the HBV-Env$^+$ mice, typically, serum transaminases were elevated no more than 2-fold above background, which is a clinically significant finding in human HBV disease.

HBV-Replication$^+$ RAG$^{-/-}$ mice were treated the day before the adoptive transfer of syngeneic naïve splenocytes with 200 μg of anti-NKG2D or control IgG, and we monitored the serum ALT levels. We found that the modest rise in the serum ALT in the HBV-Replication$^+$ RAG$^{-/-}$ mice treated with control IgG was not evident in mice treated with anti-NKG2D (Fig. 5*A*). Together with this modest rise of ALTs, we observed that 3 days after the adoptive transfer, the number of IFN-γ- and IL-4-producing cells increased by 3- and 6-fold, respectively, in mice that received control IgG as compared with NKG2D-blocked mice (Fig. 5 *D* and *E*). To evaluate the role of NKG2D in acute hepatitis developed in HBV-

Replication$^+$ mice, we examined the expression of NKG2D on NK1.1$^+$ cells from HBV-Replication$^+$ RAG$^{-/-}$ mice 3 days after adoptive transfer. Just as we observed in the HBV-Env$^+$ RAG$^{-/-}$ mice, NK cells from the livers of HBV-Replication$^+$ RAG$^{-/-}$ mice had increased expression of NKG2D during acute hepatitis, as compared with RAG$^{-/-}$ mice; and the NKT cells had down-regulated NKG2D (Fig. 5 *B* and *C*).

Discussion

Collectively, our findings clearly establish a role for NKG2D in the HBV-specific, CD1d-restricted nonclassical NKT cell-mediated acute hepatitis and cytokine production seen in both the HBV-Env$^+$ RAG$^{-/-}$ and HBV-Replication$^+$ RAG$^{-/-}$ mice. These results demonstrate a role for an NKG2D–ligand interaction in NKT cell activation. NKG2D is expressed on several cell types in the liver. However, NKG2D-bearing NK cells alone, or splenocytes depleted only of NKG2D$^+$ NKT cells do not induce acute hepatitis in the HBV-Env$^+$ RAG$^{-/-}$ and HBV-Replication$^+$ RAG$^{-/-}$ mice (ref. 8 and SI Fig. 6).

A direct effect of NKG2D blockade on NKT cell activation in our studies is suggested by several lines of evidence. First, anti-NKG2D mAb treatment efficiently prevented production of IL-4, which is expressed by the HBV-activated NKT cells but not NK cells. Second, anti-NKG2D mAb treatment decreased the number of NKT cells, but not the number of NK cells, in the livers of mice with hepatitis. Finally, NKG2D receptor expression on NKT cells, and not on other cells types, is required for efficient disease induction in our transgenic model of primary HBV infection.

For these reasons, we propose a model in which nonclassical NKT cells are first activated in a HBV-specific, CD1d-restricted and NKG2D-dependent manner, leading to production of cytokines, which in turn activate NK cells. NKG2D ligand interaction can function to directly activate cells or function as a costimulatory molecule (9–11). That the activation of nonclassical NKT cells in our mouse model of HBV infection requires expression of HBV and CD1d, in addition to an NKG2D-ligand interaction, suggests that nonclassical NKT cell activation requires a CD1d-dependent signal through its T cell receptor and that NKG2D may function as a costimulatory molecule. Further studies will be required to address whether NKG2D is also important in the subsequent NK cell activation. While our studies were under review, Chen *et al.* (23) reported the ability of NKG2D blockade to diminish hepatitis in HBV-transgenic mice; however, in these experiments, induction of the disease required the injection of the mitogen Con A, which polyclonally activates all T cells and possibly other cell types such as NK cells in the host.

We detected the NKG2D ligand, RAE-1, on the surface of all hepatocytes in normal, wild-type as well as HBV transgenic mice. This constitutive expression of RAE-1 was increased on hepatocytes from the HBV-Env$^+$ RAG$^{-/-}$ mice. Unlike the HBV-Env$^+$ RAG$^{-/-}$ mice, the amount of RAE-1 on hepatocytes from the HBV-Replication$^+$ RAG$^{-/-}$ mice was not elevated compared with nontransgenic hepatocytes (data not shown). NKG2D is nonetheless necessary for the nonclassical NKT cell activation and onset of hepatitis in both the HBV-Env$^+$ RAG$^{-/-}$ mice and HBV-Replication$^+$ RAG$^{-/-}$ mice because disease was completely prevented and cytokine production was greatly diminished by anti-NKG2D blockade. Therefore, we hypothesize that the constitutive, basal levels of RAE-1 on the hepatocytes are sufficient to trigger the HBV-specific, CD1d-restricted, NKG2D-dependent, nonclassical NKT cell-mediated hepatitis. This constitutive surface expression of RAE-1 on hepatocytes is also an interesting finding, because the expression of RAE-1 family members is strictly regulated in normal cells, and little expression is found on healthy adult tissue.

Because the HBV-Env$^+$ RAG$^{-/-}$ mice have increased expression of one of the three isoforms of HBV envelope protein (large or L protein) that is retained in the endoplasmic reticulum, these mice display increased sensitivity to the cytotoxic effects of IFN-γ (22). The up-regulation of RAE-1 in the liver of these mice may be a direct or indirect consequence of increased large envelope expression. Increased expression and accumulation of envelope proteins is also one of the pathophysiologic consequences of HBV infection in humans (24). Because expression of HBV large envelope genes is zonal (6, 25), it is possible that RAE-1 is increased on some hepatocytes that have higher expression of envelope protein, but we cannot detect the increased expression of RAE-1 because these cells are a minority of the total hepatocyte population.

Our present findings reveal a mechanism by which human HBV activates the innate immune system and sets up the cytokine milieu in which the subsequent adaptive immune response develops. The question of whether HBV alerts the innate immune system and what role the innate immune system plays in HBV pathogenesis is controversial. Studies of acute HBV infection in primates and humans reveal an initial quiescent phase of ≈4–7 weeks before HBV starts to replicate vigorously, reaching levels of 10^9 to 10^{10} copies per milliliter (26–28). Activation of components of the innate immune system are likely to play a central role in control of this initial HBV burst because HBV-DNA quantity decreases by almost 90% well in advance of the appearance of an antigen-specific CD8$^+$ T cell response and hepatopathology (27–31). However, identification of the individual components of the innate immune system responsible for this rapid down-regulation of viral replication, and the mechanism of activation, has been elusive. NK cells have been implicated in this process, because there is an increase in the number of peripheral NK cells before the peak of viral replication (31). However, Northern blot and gene expression analysis of total liver RNA derived from core liver biopsies during this period have failed to reveal evidence of activation of innate immune effector pathways, leading to the hypothesis that HBV does not alert the innate immune system (32, 33).

Our current data demonstrating that nonclassical NKT cells are activated to produce cytokines in an HBV-specific, CD1d-restricted, and NKG2D-dependent manner is consistent with a role for these cells in the initial response to HBV. The finding that activation of these nonclassical NKT cells leads to a cytokine burst in the absence of overt hepatocellular injury in the HBV-Replication$^+$ mice is consistent with the usual initial subclinical presentation of HBV infection. Using real-time PCR analysis on whole liver biopsies, we, like others, cannot detect an innate immune response (the presence of T cell receptor, IL-4, or IFN-γ transcripts) in the HBV-transgenic RAG$^{-/-}$ mice 3 days after adoptive transfer of syngeneic splenocytes (SI Fig. 7). In contrast, we clearly demonstrate the presence of NKT cells (using flow cytometry) and the production of IL-4 and IFN-γ (using ELispot assays) in the eluted lymphocytes from the same livers used in the real-time PCR experiments, as depicted in Figs. 1, 3, and 5 (data not shown). Thus, our data suggest that innate immune responses to HBV infection exist, and likely have been previously unappreciated because NKT cells represent only a small fraction of the total cell mass of the liver; thus, any NKT cell transcripts are diluted by the overwhelming abundance of hepatocyte RNA.

These mouse models of HBV infection lay the foundation for directed studies analyzing the role of NKT cells, NK cells, NKG2D, and its ligands in human HBV infection. In addition, because the activation of innate effector cells has also been implicated in hepatic flares in chronic HBV infection (34), our models offer the opportunity to examine the role of NKG2D and its ligands in chronic HBV infection, and suggest possible new strategies for therapeutic intervention in this disease.

Methods

Mice and Disease Model. HBV-Env$^+$ transgenic mice: mouse lineage 107-5D [official designation Tg (Alb-1.HBV) Bri66; inbred B10.D2, H-2^d) (5) and HBV-Replication$^+$ mice: lineage 1.3.46 [official designation, Tg (HBV 1.3 genome) chi46; inbred C57BL/6H-2^b] (6)

crossed to RAG-1 $^{-/-}$ mice. HBV-Tg × Rag-1$^{-/-}$ mice (8-to 10-week-old) were intravenously injected with donor splenocytes from 6- to 10-week-old wild-type B10.D2 or C57BL/6 male mice (The Jackson Laboratory, Bar Harbor, ME), respectively. Mice were bled by tail vein at the described intervals, and sera were collected. Other mice were killed at the indicated time points, and livers were perfused or collected for histology. All mice were kept in a pathogen-free facility at University of California (San Francisco, CA).

Alanine Aminotransferase (ALT). Serum ALT was measured by the standard photometric method by using a COBAS MIRA plus autoanalyzer.

Isolation of Hepatocytes and Intrahepatic Immune Cells. To obtain hepatocytes, livers were perfused via the thoracic portion of the inferior vein cava with a commercial liver perfusion medium (GIBCO, Carlsbad, CA) for 5 min, followed by incubation in a digestion media (DMEM Low Glucose 50%/F-12 50% mixture and 0.12–0.2 mg/ml collagenase) for 8 min. Livers were cut into small pieces and filtered through a 70-μm nylon cell strainer and centrifuged at 30 × g for 3 min. Immune cells were obtained as described (8).

Flow Cytometry. Fc-block (2.4G2 anti-CD16/32 mAb) and fluorochrome-conjugated antibodies against TCRβ (H57), NK1.1 (PK136), CD1d (1B1), H-2K^d (SF1–1.1), or the appropriate isotype-matched control Ig were purchased from BD (Franklin Lakes, NJ). PE-labeled anti-NKG2D (CX5) antibody (rat IgG1 isotype) was purchased from eBioscience (San Diego, CA). Purified antibodies against RAE-1, which recognizes all known RAE-1 proteins (rat IgG2a isotype), and MULT1 were purchased from R & D Systems (Minneapolis, MN) (35). Cells were analyzed on a LSR II (BD) by using FlowJo software.

Cell Sorting. Splenocytes were stained with anti-NKG2D mAb CX5 and the negative lymphocytes isolated. In some experiments, splenocytes were costained with anti-NKG2D (CX5), anti-TCRβ (H57), and anti-NK1.1 (PK136). Cells expressing all three cell surface markers (NKG2D$^+$ NKT cells) were depleted. All flow cytometry sorting experiments showed >98% purity by using a FACS Aria cell sorter (BD).

TaqMan Quantitative RT-PCR. Quantitative (real-time) RT-PCR was carried out by using an ABI 7300 according to the manufacture's instructions. Specific primers and probes were used for HPRT (19), pan-RAE-1 (20), IFNγ, TCRβ, and IL-4.

***In Vivo* Antibodies.** A neutralizing, nondepleting rat anti-mouse NKG2D mAb, clone CX5 (rat IgG1), generated as described (19), recognizes the NKG2D extracellular domain and blocks the binding of NKG2D to its ligands. We injected i.p. 200 μg of CX5 or control rat IgG (Sigma, St. Louis, MO) per recipient mouse the day before and 4 days after the adoptive transfer of syngeneic naïve splenocytes. To deplete NK cells, but not NKT cells, from donor splenocytes, we used a depleting rabbit anti-mouse/rat asialo GM1 polyclonal antibody purchased from Cedarlane Laboratories (21). Depletion of NK cells (<0.1%) was verified by flow cytometry before the adoptive transfer was performed.

ELISpot Assay. Intrahepatic immune cells were eluted from mice at day 3 and/or day 4 after adoptive transfer. Cells were counted and immediately plated in an anti-cytokine mAb-coated 96-well microplate (ELISpot mouse IFN-γ and IL-4 kits; BD). Eight serial 2- or 3-fold dilutions were done in duplicate, per condition. Spots were counted automatically by using an AID ELISpot Reader.

Histology. Liver was fixed, embedded in paraffin, and stained with hematoxylin and eosin. Liver sections were scored by an unbiased pathologist, according to the histopathologic standard scale for assessing viral hepatitis (36).

We thank Laura Vilarinho for technical advice; Gerald Willkom and Anna Bogdanova for technical support; João P. Pereira for technical advice and manuscript comments; and William Seaman, Samuel Baron, T. S. Benedict Yen, Stewart Cooper, and Don Ganem for critically reading the manuscript. This work was supported in part by the Burroughs Wellcome Fund, the American Liver Foundation, the Cancer Research Institute, and the University of California Liver Center (San Francisco, CA) (P30-DK26743). S.V. is supported by Portuguese Foundation for Science and Technology (POCI) 2010 Grant SFRH/BD/21982/2005. L.L.L. is an American Cancer Society Research Professor, and work was supported by National Institutes of Health Grant R37 AI066897.

1. Chang TT, Gish RG, de Man R, Gadano A, Sollano J, Chao YC, Lok AS, Han KH, Goodman Z, Zhu J, *et al.* (2006) *N Engl J Med* 354:1001–1010.
2. Lai CL, Shouval D, Lok AS, Chang TT, Cheinquer H, Goodman Z, DeHertogh D, Wilber R, Zink RC, Cross A, *et al.* (2006) *N Engl J Med* 354:1011–1020.
3. Chisari FV, Ferrari C (1995) *Annu Rev Immunol* 13:29–60.
4. Ganem D, Schneider RJ (2001) in *Fields Virology* (Lippincott, Williams & Wilkins, Philadelphia).
5. Chisari FV, Filippi P, McLachlan A, Milich DR, Riggs M, Lee S, Palmiter RD, Pinkert CA, Brinster RL (1986) *J Virol* 60:880–887.
6. Guidotti LG, Matzke B, Schaller H, Chisari FV (1995) *J Virol* 69:6158–6169.
7. Mombaerts P, Iacomini J, Johnson RS, Herrup K, Tonegawa S, Papaioannou VE (1992) *Cell* 68:869–877.
8. Baron JL, Gardiner L, Nishimura S, Shinkai K, Locksley R, Ganem D (2002) *Immunity* 16:583–594.
9. Cerwenka A, Lanier LL (2001) *Immunol Rev* 181:158–169.
10. Diefenbach A, Tomasello E, Lucas M, Jamieson AM, Hsia JK, Vivier E, Raulet DH (2002) *Nat Immunol* 3:1142–1149.
11. Wu J, Song Y, Bakker AB, Bauer S, Spies T, Lanier LL, Phillips JH (1999) *Science* 285:730–732.
12. Jamieson AM, Diefenbach A, McMahon CW, Xiong N, Carlyle JR, Raulet DH (2002) *Immunity* 17:19–29.
13. Raulet DH (2003) *Nat Rev Immunol* 3:781–790.
14. Lanier LL (2005) *Annu Rev Immunol* 23:225–274.
15. Carayannopoulos LN, Naidenko OV, Fremont DH, Yokoyama WM (2002) *J Immunol* 169:4079–4083.
16. Cerwenka A, Bakker AB, McClanahan T, Wagner J, Wu J, Phillips JH, Lanier LL (2000) *Immunity* 12:721–727.
17. Diefenbach A, Jamieson AM, Liu SD, Shastri N, Raulet DH (2000) *Nat Immunol* 1:119–126.
18. Gasser S, Orsulic S, Brown EJ, Raulet DH (2005) *Nature* 436:1186–1190.
19. Ogasawara K, Hamerman JA, Hsin H, Chikuma S, Bour-Jordan H, Chen T, Pertel T, Carnaud C, Bluestone JA, Lanier LL (2003) *Immunity* 18:41–51.
20. Ogasawara K, Hamerman JA, Ehrlich LR, Bour-Jordan H, Santamaria P, Bluestone JA, Lanier LL (2004) *Immunity* 20:757–767.
21. Seki S, Hashimoto W, Ogasawara K, Satoh M, Watanabe H, Habu Y, Hiraide H, Takeda K (1997) *Immunology* 92:561–566.
22. Gilles PN, Guerrette DL, Ulevitch RJ, Schreiber RD, Chisari FV (1992) *Hepatology* 16:655–663.
23. Chen Y, Wei H, Sun R, Dong Z, Zhang J, Tian Z (2007) *Hepatology* 46:706–715.
24. Davies SE, Portmann BC, O'Grady JG, Aldis PM, Chaggar K, Alexander GJ, Williams R (1991) *Hepatology* 13:150–157.
25. Hollinger FB, Liang TJ (2001) in *Fields Virology* (Lippincott, Williams & Wilkins, Philadelphia).
26. Whalley SA, Murray JM, Brown D, Webster GJ, Emery VC, Dusheiko GM, Perelson AS (2001) *J Exp Med* 193:847–854.
27. Guidotti LG, Rochford R, Chung J, Shapiro M, Purcell R, Chisari FV (1999) *Science* 284:825–829.
28. Bertoletti A, Ferrari C (2003) *Hepatology* 38:4–13.
29. Jilbert AR, Wu TT, England JM, Hall PM, Carp NZ, O'Connell AP, Mason WS (1992) *J Virol* 66:1377–1388.
30. Kajino K, Jilbert AR, Saputelli J, Aldrich CE, Cullen J, Mason WS (1994) *J Virol* 68:5792–5803.
31. Webster GJ, Reignat S, Maini MK, Whalley SA, Ogg GS, King A, Brown D, Amlot PL, Williams R, Vergani D, *et al.* (2000) *Hepatology* 32:1117–1124.
32. Wieland S, Thimme R, Purcell RH, Chisari FV (2004) *Proc Natl Acad Sci USA* 101:6669–6674.
33. Wieland SF, Chisari FV (2005) *J Virol* 79:9369–9380.
34. Dunn C, Brunetto M, Reynolds G, Christophides T, Kennedy PT, Lampertico P, Das A, Lopes AR, Borrow P, Williams K, *et al.* (2007) *J Exp Med* 204:667–680.
35. Lodoen M, Ogasawara K, Hamerman JA, Arase H, Houchins JP, Mocarski ES, Lanier LL (2003) *J Exp Med* 197:1245–1253.
36. Scheuer PJ (1991) *J Hepatol* 13:372–374.

Th1 and Type 1 Cytotoxic T Cells Dominate Responses in T-bet Overexpression Transgenic Mice That Develop Contact Dermatitis[1]

Kazusa Ishizaki,[2]* Akiko Yamada,[2]* Keigyou Yoh,[‡] Takako Nakano,* Homare Shimohata,* Atsuko Maeda,* Yuki Fujioka,* Naoki Morito,* Yasuhiro Kawachi,[§] Kazuko Shibuya,[†] Fujio Otsuka,[§] Akira Shibuya,[†] and Satoru Takahashi[3]*

Contact dermatitis in humans and contact hypersensitivity (CHS) in animal models are delayed-type hypersensitivity reactions mediated by hapten-specific T cells. Recently, it has become clear that both $CD4^+$ Th1 and $CD8^+$ type 1 cytotoxic T (Tc1) cells can act as effectors in CHS reactions. T-bet has been demonstrated to play an important role in Th1 and Tc1 cell differentiation, but little is known about its contribution to CHS. In the present study, we used C57BL/6 mice transgenic (Tg) for T-bet to address this issue. These Tg mice, which overexpressed T-bet in their T lymphocytes, developed dermatitis characterized by swollen, flaky, and scaly skin in regions without body hair. Skin histology showed epidermal hyperkeratosis, neutrophil, and lymphocyte infiltration similar to that seen in contact dermatitis. T-bet overexpression in Tg mice led to elevated Th1 Ig (IgG2a) and decreased Th2 Ig (IgG1) production. Intracellular cytokine analyses demonstrated that IFN-γ was increased in both Th1 and Tc1 cells. Furthermore, Tg mice had hypersensitive responses to 2,4-dinitrofluorobenzene, which is used for CHS induction. These results suggest that the level of expression of T-bet might play an important role in the development of contact dermatitis and that these Tg mice should be a useful model for contact dermatitis. *The Journal of Immunology,* **2007, 178: 605–612.**

The Th1/Th2 paradigm proposed by Mosmann et al. (1) holds that $CD4^+$ T cells can be subdivided into two categories, namely Th1 and Th2 (2). These two polarized subsets can be identified on the basis of the cytokines they secrete (3). Th1 cells produce IL-2 and IFN-γ, whereas Th2 cells produce IL-4, IL-5, IL-6, IL-10, and IL-13. More recently, a similar heterogeneity among $CD8^+$ T cytotoxic (Tc)[4] cells has also been recognized with the identification of Tc1 and Tc2 subpopulations (4, 5). IFN-γ is also one of the main cytokines produced by differentiated $CD8^+$ effector T cells and has been shown to have a fundamental role in $CD8^+$ T cell-mediated immunity (6). Lineage commitment of $CD4^+$ and $CD8^+$ T cells is transcriptionally regulated, often by the same factors that mediate T cell effector function.

T-bet is known as a Th1 lineage commitment transcription factor as a result of its transactivation of the Th1 cytokine IFN-γ (7). Recently, T-bet has also been shown to regulate cytolytic effector mechanisms of $CD8^+$ T cells (8). T-bet expression is rapidly induced in $CD8^+$ T cells by signaling through the TCR and the IFN-γR, and it functions downstream of STAT1 (6, 9, 10). In the context of Ag-specific activation, T-bet is required for the differentiation of naive $CD8^+$ T cells into effector CTLs.

Contact dermatitis is one of the most common skin diseases (11). Knowledge of the pathophysiology of contact dermatitis is derived chiefly from animal models in which the inflammation induced by hapten painting of the skin is referred to as contact hypersensitivity (CHS) (12). Contact dermatitis and CHS are delayed-type hypersensitivity reactions that are mediated by hapten-specific T cells (12). Skin sensitization resulting in contact dermatitis and CHS is dependent on the initiation of specific T lymphocyte responses (11, 13). Until recently it was believed that the most important cells in these responses were $CD4^+$ T lymphocytes. IL-2 and IFN-γ produced by Th1 cells are thought to play a preeminent role in the evolution of CHS (14, 15). Some investigations in mice found CHS to be associated with $CD4^+$ T lymphocyte function and to be compromised when such cells were deleted (15, 16). However, there is growing evidence that in many instances the predominant effector cell in CHS may be a $CD8^+$ T lymphocyte (13, 17, 18). Wang et al. (17) clearly demonstrated that the deletion of $CD8^+$ Tc1 cells had a more significant suppressive effect than the deletion of $CD4^+$ Th1 cells in CHS responses to 2,4-dinitrofluorobenzene (DNFB). According to these results, both $CD4^+$ Th1 and $CD8^+$ Tc1 cells are key players in CHS.

Although T-bet plays an important role in Th1 and Tc1 cell induction, little is known about its contribution to CHS. In the present study we used T-bet overexpression in T cell transgenic (Tg) mice to address this issue.

*Department of Anatomy and Embryology, †Department of Immunobiology, Biomolecular, and Integrated Medical Sciences, ‡Department of Pathophysiology of Renal Diseases, and §Department of Dermatology, Medical Sciences for Control of Pathological Processes, Graduate School of Comprehensive Human Sciences, University of Tsukuba, Ibaraki, Japan

Received for publication March 10, 2006. Accepted for publication October 12, 2006.

The costs of publication of this article were defrayed in part by the payment of page charges. This article must therefore be hereby marked *advertisement* in accordance with 18 U.S.C. Section 1734 solely to indicate this fact.

[1] This work was supported by Grants-in-Aid for Young Scientists (B) and Scientific Research (C) from the Ministry of Education, Science, Sports, and Culture and a grant of the Genome Network Project from the Ministry of Education, Culture, Sports, Science, and Technology, Japan.

[2] K.I. and A.Y. contributed equally to this work.

[3] Address correspondence and reprint requests to Dr. Satoru Takahashi, Department of Anatomy and Embryology, Biomolecular, and Integrated Medical Sciences, Graduate School of Comprehensive Human Sciences, University of Tsukuba, 1-1-1 Tennodai, Tsukuba, Ibaraki, 305-8575, Japan. E-mail address: satoruta@md.tsukuba.ac.jp

[4] Abbreviations used in this paper: Tc, cytotoxic T; CHS, contact hypersensitivity; DNFB, 2,4-dinitrofluorobenzene; LNC, lymph node cell; Tg, transgenic; WT mice, wild-type transgene-negative littermates.

Materials and Methods

Generation of T-bet Tg mice

A 2.5-kb, full-length cDNA encoding the murine T-bet protein was inserted into a VA CD2 transgene cassette containing the upstream gene regulatory region and locus control region of the human CD2 gene. The VA vector has been reported to direct expression of the inserted cDNA in all single-positive mature T lymphocytes of Tg mice, with expression being linearly proportional to the transgene copy number (19). This T-bet construct was injected into BDF1 fertilized eggs to generate Tg mice. T-bet Tg mice were inbred with C57BL/6 mice for four generations. Mice were maintained in specific pathogen-free conditions in a laboratory animal resource center. All experiments were performed according to the Guide for the Care and Use of Laboratory Animals at the University of Tsukuba (Ibaraki, Japan), and the study was approved by the Institutional Review Board of the university.

Southern hybridization analysis of genomic DNA

Southern hybridization was performed by using the Gene Images random prime labeling module system (Amersham Biosciences). High m.w. DNA was prepared from the tail of each mouse, and 15 μg of DNA was digested with *ApaI* and then subjected to electrophoresis on 1.0% agarose gels. After electrophoresis, the DNA was transferred to a Hybond-N^+ membrane. A fluorescence-labeled *ApaI/KpnI* fragment (0.5 kb) of the *T-bet* cDNA was used as a probe. The transgene copy number was determined from the blot with a BAS 1500 Mac image analyzer.

RT-PCR for transgene expression analysis

Total RNA was prepared from the thymus of 10 wk-old Tg mice or their wild-type transgene-negative littermates (WT mice) using TRIzol reagent according to the manufacturer's instructions (Invitrogen Life Technologies). First-strand cDNA was synthesized at 42°C for 50 min using the SuperScript II RNase H2 reverse-transcriptase kit (Invitrogen Life Technologies), and 1 μl of this 20 μl reaction mixture was used for the PCR. Amplified products were analyzed on 2% agarose gels. PCR primer sequences were as follows: T-bet, 5′-CGGTACCAGAGCGGCAAGT-3′ and 5′-AGCCCCCTTGTTGTTGGTG-3′; GATA-3, 5′-TCTCACTCTCGAG GCAGCATGA-3′ and 5′-GGTACCATCTCGCCGCCACAG-3′; GAPDH, 5′-CCCCTTCATTGACCTCAACTACATGG-3′ and 5′-GCCTGCTTCAC CACCTTCTTGATGTC-3′.

Western blot analysis

Thymocyte nuclear extracts were prepared from 10 wk-old Tg mice or WT. The extracts were size-fractionated on a 10% SDS-polyacrylamide gel, transferred to a polyvinylidene difluoride membrane (FluoroTrans), and reacted with primary and secondary Abs. For detection of the T-bet protein, a goat anti-mouse T-bet (N-19; Santa Cruz Biochemicals) was used as the primary Ab and peroxidase-conjugated rabbit anti-goat IgG (Zymed Laboratories) was used as the secondary Ab. For normalization with respect to the amount of protein in each sample, anti-lamin B Ab (Santa Cruz Biochemicals) was used as a control.

Histopathological analysis

Organs were fixed with 10% formalin in 0.01 M phosphate buffer (pH 7.2) and embedded in paraffin. Sections (3 μm) were stained with H&E for histopathological examination by light microscopy.

Measurement of serum Ig

Total serum Ig was determined by ELISA as previously described (20). Briefly, Nunc immunoplates were coated with goat anti-mouse Ig (ICN Pharmaceuticals). The plates were kept at room temperature for 1 h and then washed with 0.1 M PBS. After washing, the plates were blocked with 0.5% BSA in PBS solution. Serial dilutions of test serum samples were applied and incubated at room temperature for 1 h. After washing with PBS, the plates were treated with alkaline phosphatase-conjugated goat anti-mouse IgG, IgG1, or IgG2a (Sigma-Aldrich) at room temperature for 1 h. After additional washes, alkaline phosphatase substrate (Sigma-Aldrich) solution was added and allowed to develop. Absorption at 405 nm was measured with an immunoplate reader (BenchMark; Bio-Rad).

Culture medium, cytokines, and Abs

RPMI 1640 medium supplemented with 10% FCS, 2-ME (0.05 mM), L-glutamine (2 mM), penicillin (100 U/ml), streptomycin (100 μg/ml), HEPES buffer (10 mM), and sodium pyruvate (1 mM) was used as culture medium. Recombinant mouse cytokines were IL-2 (Genzyme Techne), IL-4 (BD Pharmingen), and IL-12 (BD Pharmingen). Purified rat anti-mouse IL-4 (11B11), IL-12 (C17.8), CD3e (145-2C11), and CD28 (37.51) mAb, PE-conjugated anti-mouse IL-5 (TRFK5), and FITC-conjugated anti-mouse IFN-γ (XMG1.2) were purchased from BD Pharmingen.

Preparation of T Cells

$CD4^+$ and $CD8^+$ T cells were prepared from each mouse spleen and lymph nodes. $CD4^+$ and $CD8^+$ T cells were enriched by positive selection using a MACS system with anti-CD4 and anti-CD8 mAb (Miltenyi Biotec). In the spleen cell transfer experiment the cells (3×10^6 cells) were transferred i.v.

Stimulation of Tg $CD4^+CD8^+$ T cells for cytokine production

Primary stimulations of $CD4^+/CD8^+$ T cells (2.5×10^5 cells/well) were performed with cross-linked anti-CD3e (1 μg/ml) and anti-CD28 (10 μg/ml) plus IL-2 (10 ng/ml) in a total volume of 2 ml in 24-well plates. In addition, some cultures received cytokines (10 ng/ml IL-4 or 10 ng/ml IL-12) or mAb to block endogenous cytokines (10 μg/ml anti-IL-4 or 10 μg/ml anti-IL-12). T cells were expanded and maintained under constant culture conditions for 1 wk.

Flow cytometric analysis of intracellular IL-5 and IFN-γ synthesis

Cells were resuspended at 10^5 to 10^6 cells/ml and stimulated with PMA (50 ng/ml) plus ionomycin (500 ng/ml). Two hours before cell harvesting, brefeldin A was added at 10 μg/ml using a stock solution of 1 mg/ml in ethanol (100%). Cells were harvested, washed, and resuspended in PBS with brefeldin A before the addition of an equal volume of 4% formaldehyde fixative (final concentration, 2%). After fixation for 20 min at room temperature, cells were stained for cytokines. For intracellular staining, all reagents and washes contained 1% BSA and 0.5% saponin (Sigma-Aldrich), and all incubations were performed at room temperature. Cells were washed and preincubated for 10 min in PBS/BSA/saponin and then incubated with allophycocyanin-conjugated anti-mouse IL-5 (5 μg/ml) and anti-mouse IFN-γ (5 μg/ml) or isotype-matched control Abs (10 μg/ml) for 30 min. After 20 min, cells were washed twice with PBS/BSA/saponin and then washed with PBS/BSA without saponin to allow membrane closure. Samples were analyzed with a FACScalibur flow cytometer (BD Biosciences). Results were analyzed by using CellQuest software.

Induction of CHS

Induction of CHS was conducted using the methods described previously (21). Briefly, mice were sensitized to DNFB by painting the shaved abdomen with 50 μl of 0.5% DNFB in acetone/olive oil (4:1) and each footpad with 5 μl of the mixture on days 0 and 1. On day 5, mice were challenged with 20 μl of 0.3% DNFB on each side of the left ear. As a control, the right ear was painted with an identical amount of vehicle. The ear thickness was measured at 12, 24, 48, and 72 h after challenge at three locations. The ear swelling was calculated as $[(T - T_0)$ left ear$] - [(T - T_0)$ right ear], where T_0 and T represent the values of ear thickness before and after the challenge, respectively.

Results

Generation of Tg mouse lines overexpressing T-bet in T cells

To generate Tg mouse lines expressing high levels of T-bet specifically in T cells, the mouse *T-bet* cDNA was inserted into the VA vector (Fig. 1*A*). Genomic Southern blotting analysis was performed to confirm the integrity and copy number for each Tg mouse line. The length of the *ApaI* fragment containing the *T-bet* transgene was 1.2 kb, whereas the corresponding fragment for the endogenous *T-bet* gene was 4.0 kb (Fig. 1*A*). The transgene was detected in mice of Tg lines 710, 725, and 731 (Fig. 1*B*). In densitometric analyses, line 710 seemed to contain more than 12 copies of the transgene, whereas lines 725 and 731 contained approximately 12 and 8 copies, respectively. However, line 710 could not transmit the genes to the next generation, but the transgenes in both line 725 and line 731 were stably transmitted to progeny.

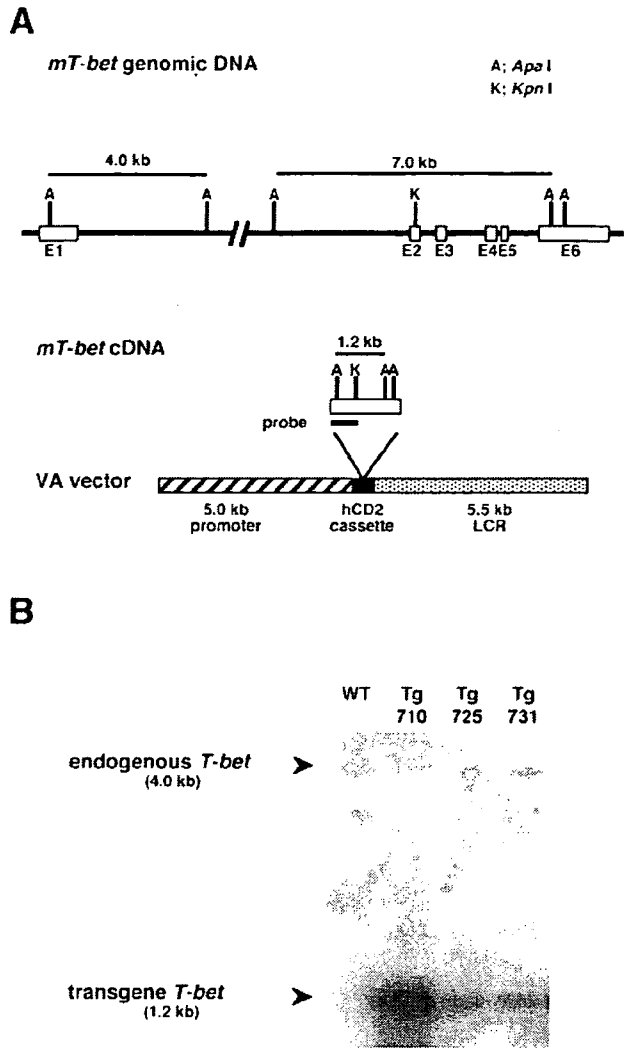

FIGURE 1. Generation of T-bet-overexpressing mice. *A*, Diagram showing the structures of the mouse *T-bet* (*mT-bet*) gene locus and the Tg construct. *T-bet* cDNA was inserted into a vector (VA vector) containing a human CD2 transgene cassette. The Southern blotting probe site, the restriction sites, and the predicted sizes of the endogenous gene and the transgene (with *Apa*I restriction sites) are indicated. E, Exon; LCR, locus control region. *B*, Southern blot analysis of the endogenous and Tg *T-bet* genes in Tg mice. The fragment with *Apa*I and *Kpn*I restriction sites in *mT-bet* cDNA in panel (*A*) was used as the probe. The 4.0-kb endogenous and 1.2-kb Tg genes are shown for Tg line 710 (Tg 710), Tg 725 (Tg 725), and Tg 731 (Tg 731) mice. The transgene copy numbers for Tg lines 710, 725, and 731 were over 12, 12, and 8 copies, respectively.

Overexpression of T-bet in Tg mice

To confirm expression of the transgene, RT-PCR and immunoblot analyses were performed to monitor T-bet mRNA and protein levels in thymocytes from the two Tg lines (Fig. 2, *A* and *B*). Overexpression of T-bet mRNA and protein was detected in all Tg mice tested. The amount of T-bet protein in Tg line 725 cells was slightly higher than the amount in Tg line 731, indicating that the expression level of the protein was copy number dependent. The T-bet protein was not detected in WT mice in this analysis.

Higher ratio between IgG2a and IgG1 in T-bet Tg mice

To determine cytokine levels we first analyzed serum by the ELISA method, but all samples were below the level of detection (data not shown). Because Th1/Th2 cytokines contribute to control of Ig subtype production, we next analyzed serum IgG1 and IgG2a. Th1 cells support macrophage activation, delayed-typed hypersensitivity responses, and Ig isotype switching to IgG2a. In contrast, Th2 cells provide efficient help for B cell activation and class switching to IgG1 (22, 23). To confirm the Th1-dominant response in T-bet Tg mice, serum IgG levels were measured by ELISA (Table I). Tg line 731 mice had serum total IgG levels similar to those of WT mice (Tg line 731, 394.0 ± 37.6 mg/dl; WT, 340.3 ± 18.7 mg/dl), but Tg line 725 levels were significantly higher than those of WT mice (547.4 ± 108.9 mg/dl). Serum IgG1 levels of Tg mice (Tg line 731, 79.4 ± 7.4 mg/dl) tended to be lower than those of WT mice (174.0 ± 33.7 mg/dl) but, in contrast, IgG2a levels were higher (Tg line 725, 253.1 ± 77.9 mg/dl; WT, 90.7 ± 12.6 mg/dl). To confirm the promotion of the IgG2a class switch and repression of IgG1 Tg mice, IgG2a/IgG1 ratios were calculated. These were found to be significantly higher in Tg mice (Tg line 725, 2.93 ± 0.95; Tg line 731, 1.22 ± 0.13) than in WT mice (0.62 ± 0.08) ($p < 0.01$).

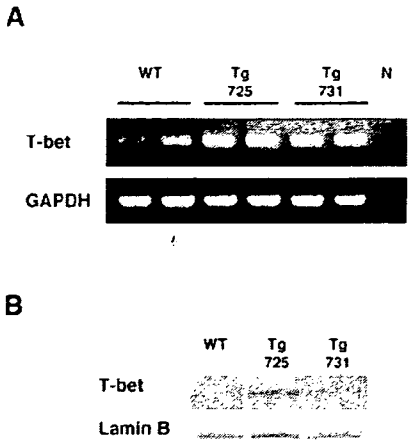

FIGURE 2. T-bet expression analysis by RT-PCR and Western blot in the thymus. *A*, RT-PCR analysis. In Tg line 725 (Tg 725) and Tg line 731 (Tg 731), T-bet gene expression was higher than that of WT. N, PCR without template as negative control. Two individual mice were used in each genotype. *B*, T-bet protein in nuclear extracts from thymocytes. T-bet protein was clearly identified by Western blotting in the extracts from Tg lines 725 and 731. In this analysis, however, the normal level of T-bet from WT thymocytes could not be detected.

Increased synthesis of IFN-γ in T-bet Tg mice

From the above data, Tg line 725 mice had greater overexpression of T-bet than Tg line 731 mice and were therefore used in the following studies. To confirm the observed differences in

Table I. *Serum immunoglobulins for 30-week-old mice*[a]

Measurement	WT (n = 12)	Tg Line 725 (n = 8)	Tg Line 731 (n = 10)
IgG (mg/dl)	340.3 ± 18.7	547.4 ± 108.9[b]	394.0 ± 37.6
IgG1 (mg/dl)	174.0 ± 33.7	174.9 ± 89.0	79.4 ± 7.4[b]
IgG2a (mg/dl)	90.7 ± 12.6	253.1 ± 77.9[b]	97.1 ± 13.4
IgG2a/IgG1 ratio	0.62 ± 0.08	2.93 ± 0.95[c]	1.22 ± 0.13[c]

[a] Data are expressed as mean ± SEM.
[b] $p < 0.05$ versus WT.
[c] $p < 0.01$ versus WT.

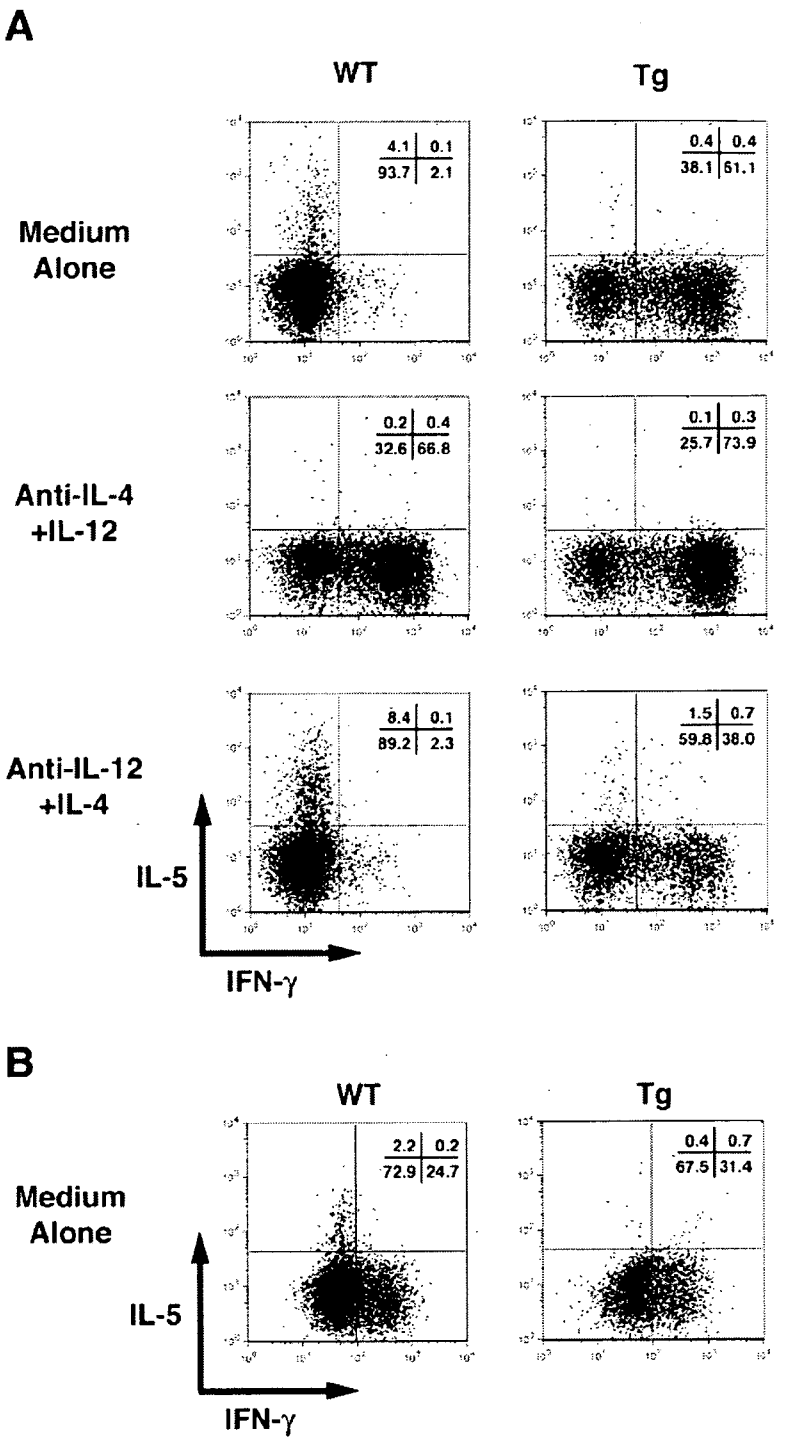

FIGURE 3. Intracellular cytokine analysis of $CD4^+$ (*A*) and $CD8^+$ (*B*) T cells from each group. *A*, $CD4^+$ T cells from WT and Tg line 725 mice were cultured in the presence of medium alone, anti-IL-4 plus IL-12 (Th1 differentiation conditions), or anti-IL-12 plus IL-4 (Th2 differentiation conditions) and analyzed by flow cytometry for intracellular synthesis of IFN-γ and IL-5. The frequencies of IFN-γ-producing cells are shown on the *x*-axis and those of IL-5-producing cells on the *y*-axis. Intracellular synthesis of IFN-γ in Tg line 725 mice was increased under all conditions. *B*, $CD8^+$ T cells from WT and Tg line 725 mice were cultured in the presence of medium alone and analyzed by flow cytometry for intracellular synthesis of IFN-γ and IL-5. Results are representative of three independent experiments.

cytokine production at the single-cell level, we studied their intracellular synthesis by flow cytometry. $CD4^+$ T cells from Tg mice had higher levels of IFN-γ than WT mice either in medium alone or under conditions favoring Th1 differentiation (presence of anti-IL-4 Ab and IL-12) or Th2 differentiation (presence of anti-IL-12 Ab and IL-4) (Fig. 3*A*). Especially in the Th2 condition 38.0% of $CD4^+$ T cells from Tg mice produced IFN-γ, but only 2.3% from WT did so. In contrast to IFN-γ, the production of IL-5 in cells from Tg mice showed lower levels in medium and the Th2 condition. IL-4 production

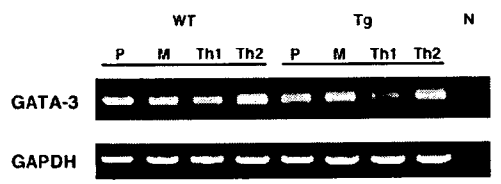

FIGURE 4. GATA-3 mRNA expression analysis by RT-PCR in intracellular cytokine production experiment. P, Prestimulation; M, medium-alone condition; Th1, Th1 differentiation conditions; Th2, Th2 differentiation conditions; N, PCR without template as negative control.

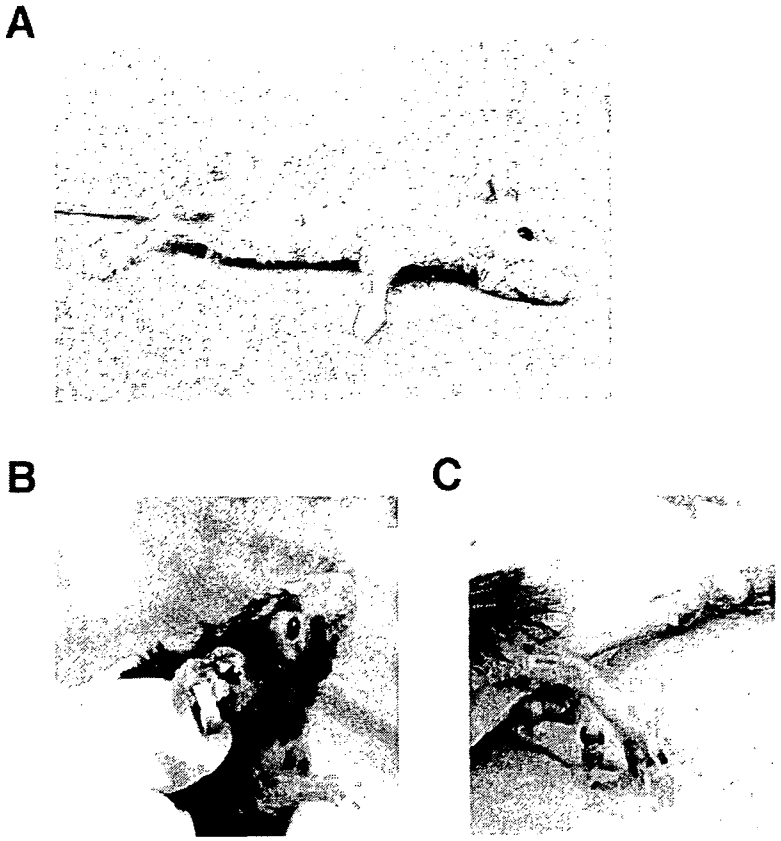

FIGURE 5. Tg mice develop dermatitis. In severe cases, individual Tg mice lost hair all over the body (*A*). In mild cases, the surface of the face, ear, foot, and tail showed redness and scaling (*B* and *C*).

analyses were also done. IL-4 production in cells from Tg and WT mice was similar and the percentage of positive cells was very low under all conditions (data not shown). These results demonstrate that T cells from T-bet Tg mice have a dominant Th1 differentiation pattern and suggest that overexpression of T-bet prevents Th2 differentiation. $CD8^+$ T cells from Tg mice also had higher levels of IFN-γ than WT mice in neutral condition, but not so markedly as that of $CD4^+$ T cells from Tg mice (Fig. 3*B*). We also determined the GATA-3 mRNA expression in the intracellular cytokine production analyses (Fig. 4). GATA-3 mRNA expression in Tg mice showed lower levels than those of wild mice, especially in a Th1 condition.

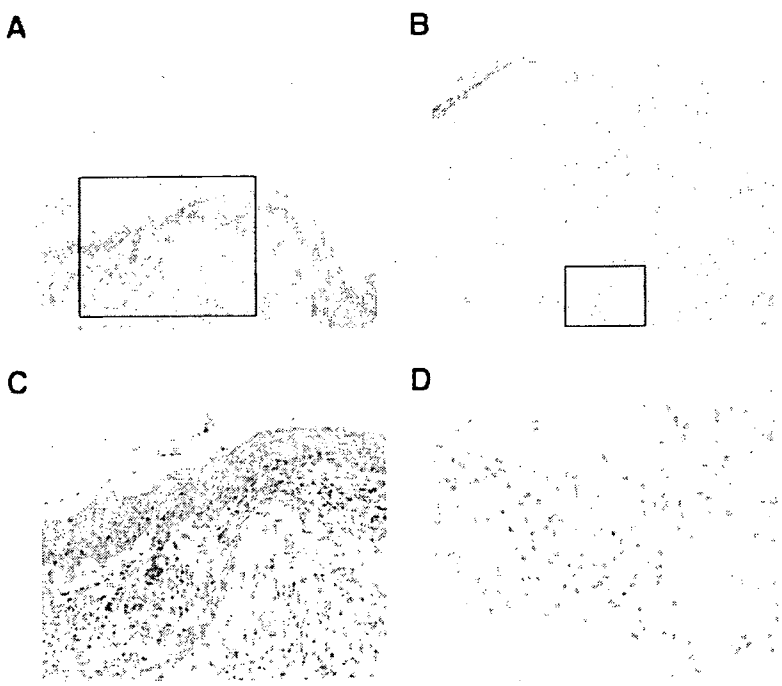

FIGURE 6. Histological appearance of the ear skin. *A* and *B*, In the histological analysis of ear skin, hyperkeratosis, acanthosis, broadening of the papillae, and infiltration of neutrophils lymphocytes, and melanophages are seen. *C and D*, At higher magnification of the squares from *A* and *B*, infiltration of mononuclear cells and neutrophils is observed. (H&E staining; magnification: ×100 (*A*), ×100 (*B*), ×200 (*C*), and ×400 (*D*).

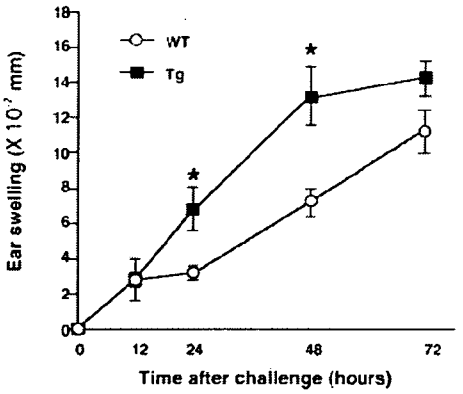

FIGURE 7. CHS reaction to DNFB in Tg and WT mice. The CHS response was determined by ear swelling at various times after hapten challenge. Time after challenge was 24 and 48 h; the ear swelling values in Tg mice (■, $n = 5$) were significantly higher than those in WT mice (○, $n = 5$). *, $p < 0.05$.

Development of contact dermatitis in T-bet Tg mice

During the initial analysis of the Tg cohorts we found that they developed dermatitis. At ~10 wk of age, ~28% of Tg line 725 (12 of 43) and 5% of Tg line 731 (3 of 61) mice spontaneously developed dermatitis characterized by swollen, flaky, and scaly skin in regions lacking body hair (e.g., tail or ears), which in some individuals progressed all over the body, together with alopecia (Fig. 5). Histological examination of the affected skin showed epidermal hyperkeratosis and neutrophil and lymphocyte infiltration similar to what is seen in contact dermatitis in humans (Fig. 6). To prove that the skin lesion was contact dermatitis although the Ag was not determined, we performed cell transfer experiment. We transferred total spleen cells from T-bet to WT mice and found that dermatitis was induced in 70% (7 of 10 mice) within one month. However, dermatitis was not observed after the transfer of separated $CD4^+$ or $CD8^+$ cells alone.

Augmentation of CHS reactions in Tg mice

To determine the role of T-bet overexpression in T cell subpopulations in CHS responses, 6-wk-old WT and Tg (Tg line 725) mice, which did not develop dermatitis, were sensitized with DNFB as described in *Materials and Methods*. Ear swelling responses to DNFB were significantly increased in Tg mice compared with WT mice (Fig. 7). The CHS response was significantly higher at 24 and 48 h after challenge. Histological analysis of hapten-treated WT and Tg ears showed characteristic features of CHS including dermal edema, mononuclear cell infiltration, and vascular enlargement (Fig. 8*B*). These histological changes were dramatically enhanced in hapten-treated Tg mouse ears (Fig. 8*B*).

Both $CD4^+$ and $CD8^+$ T cell lymph node cells (LNCs) produce significant amounts of IFN-γ in T-bet Tg mice

To determine IFN-γ production in skin-draining lymph nodes of Tg and WT mice, DNFB-primed LNCs were cultured under condition with medium alone. A significant increase of IFN-γ-producing cells was found among both $CD4^+$ and $CD8^+$ LNCs from DNFB-stimulated Tg mice (Fig. 9). In Tg mice, IFN-γ-producing cells were increased in $CD4^+$ LNCs even without DNFB stimulation. After stimulation, IFN-γ-producing cells increased further (Fig. 9*A*). Regarding $CD8^+$ LNCs, WT and Tg mice had the similar levels of IFN-γ-producing cells, but after DNFB stimulation the increase of IFN-γ-producing cells was greater in Tg mice (Fig. 9*B*). IL-10 production was also analyzed as a marker cytokine of

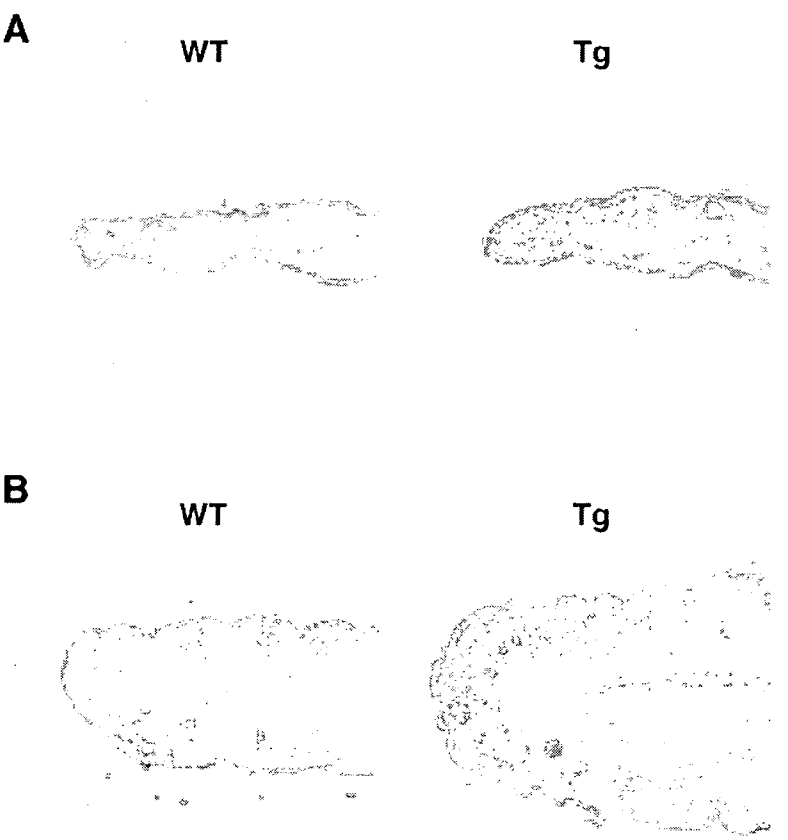

FIGURE 8. Representative results from histological analysis of CHS reactions. At 72 h after challenge, skin sections are shown from vehicle-treated mice (*A*) and hapten-treated mice (*B*) (H&E staining; magnification: ×100). *A*, Sections from vehicle-treated Tg mice exhibited normal histological features similar to those of vehicle-treated WT mice. *B*, Sections from hapten-treated WT and Tg mice displayed characteristic features of the CHS reaction including dermal edema, mononuclear cell infiltration, and vascular enlargement (*B*). The severity of the CHS reaction was greater in Tg mice.

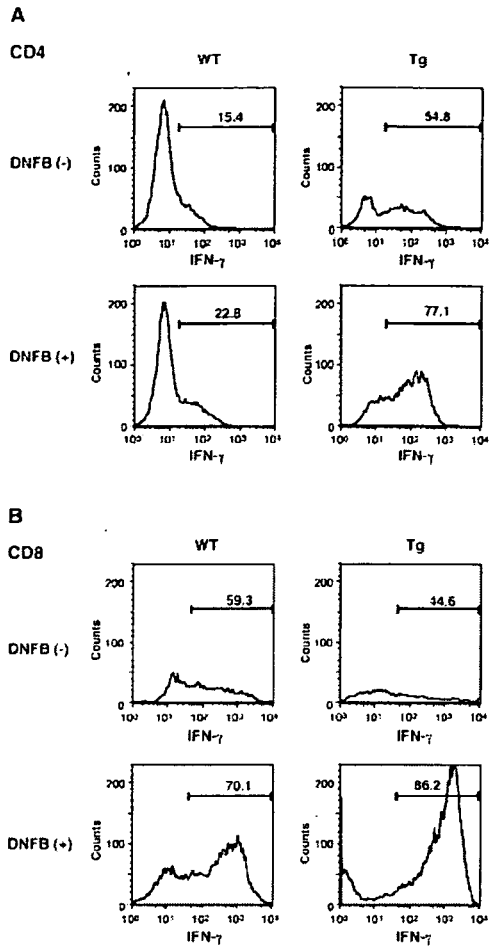

FIGURE 9. The number of IFN-γ-producing cells among $CD4^+$ and $CD8^+$ T cells was increased in CHS-sensitized Tg LNCs. LNCs from 72 h DNFB-sensitized or non-sensitized WT and Tg mice were cultured in medium alone and subjected to intracellular cytokine staining as described in *Materials and Methods*. Significantly higher numbers of IFN-γ-producing cells were detected in DNFB-sensitized Tg $CD4^+$ (*A*) and $CD8^+$ (*B*) T cells. Results are representative of three independent experiments.

Th2 or Tc2. However, no significant differences between Tg and WT mice were found (data not shown).

Discussion

T-bet is known as a master regulator of Th1 development. It induces IFN-γ production and repression of Th2 cytokines in vitro (7). In this study, we generated T-bet-overexpressing mice characterized by Th1-dominant responses in vivo and in vitro. Thus, T-bet Tg mice showed Th1-dominant Ig production in vivo and Th1-dominant intracellular cytokine production in vitro. Because serum cytokines were below the level of detection, we analyzed serum Ig isotypes. IFN-γ promotes IgG2a class switching while IL-4 promotes IgG1 class switching, so concentrations of serum IgG2a and IgG1 reflect Th1 and Th2 responses in vivo (22–24). The higher IgG2a/IgG1 ratio present in the sera of Tg mice suggests that T-bet overexpression promotes IgG2a class switching and represses IgG1 class switching. At the same time, we analyzed intracellular cytokines and found that $CD4^+$ T cells from Tg mice produced higher levels of IFN-γ than WT mice under neutral, Th1- or Th2-promoting conditions. In contrast, IL-5 production in $CD4^+$ T cells from Tg mice was lower than that in $CD4^+$ T cells from WT mice under neutral or Th2-promoting conditions. The serological Ig findings are therefore consistent with data from $CD4^+$ T cell intracellular cytokine assays, emphasizing that these do indeed reflect the Th1/Th2 balance in vivo. T-bet has also been shown to regulate cytolytic effector mechanisms of $CD8^+$ T cells (8). Its expression is rapidly induced in $CD8^+$ T cells by signaling through the TCR and the IFN-γR, and it functions downstream of STAT1 (6, 9, 10). In the context of Ag-specific activation, T-bet is required for the differentiation of naive $CD8^+$ T cells into effector CTLs. In the present study, Tg mice also had a higher fraction of IFN-γ-producing $CD8^+$ T cells according to intracellular cytokine assays, but not as markedly as $CD4^+$ T cells. However, Tg mice showed higher response for IFN-γ-producing $CD8^+$ T cells in the CHS response. From the above results, we speculated that Tg mice not only had a Th1-dominant background but also a potential Tc1-dominant background.

In this study, spontaneous skin inflammation was observed in Tg mice, first occurring in regions lacking body hair such as the tail or ears, where the skin is easily in contact with external agents. Histological examination of affected skin showed epidermal hyperkeratosis, spongiosis, and neutrophil and lymphocyte infiltration. This is typical for contact dermatitis, a delayed-type hypersensitivity reaction. It is known that Th1 activity greatly contributes to the development of dermatitis (25, 26). It is shown here that a Th1-dominant response occurs in T-bet Tg mice. Tg mice expressing IFN-γ in the epidermis have also been investigated previously and found to have reddened skin, growth retardation, hair loss, and flaky skin lesions (25). Keratinocyte proliferation was increased and there was epidermal thickening with spongiosis and parakeratosis. The possible importance of several cytokines such as IL-2 (27), IL-6 (28), and IL-7 (29) in the development of contact dermatitis has also been investigated using Tg mouse models (30). In this study we used Tg mice overexpressing the T cell differentiation transcription factor T-bet, but not cytokine transgenes, to address contact dermatitis for the first time. The results from this study suggested that transcriptional regulation of T-bet might play an important role in contact dermatitis.

Contact allergens such as DNFB, oxazolone, and 2,4-dinitrochlorobenzene are used to induce CHS. In the present study we also showed that Tg mice responded significantly to DNFB. There have been major controversies on the respective roles of $CD4^+$ and $CD8^+$ T cells in the development of CHS inflammatory reactions (12). However, it has become clear that both $CD4^+$ and $CD8^+$ T cells can act as effector cells in this context (17). Wang et al. (17) showed that both $CD4^+$ Th1 and $CD8^+$ Tc1 cells are crucial effectors in the CHS response to DNFB. Previous studies have also demonstrated that cytokines play important effector and regulatory roles in CHS responses. The type 1 cytokine IFN-γ promotes CHS, whereas type 2 cytokines down-regulate CHS responses (31–33). It has been demonstrated that type 1 cytokines can be produced by $CD8^+$ Tc1 cells as well as by $CD4^+$ Th1 cells in the same way that type 2 cytokines can be derived from Th2 and Tc2 cells (5, 34). Intracellular cytokine analyses showed that T-bet-overexpressing Tg mice had a large fraction of IFN-γ-positive cells within both $CD4^+$ and $CD8^+$ T cells. We also transferred total spleen cells from T-bet to WT mice and found that dermatitis was induced in 70% (7 of 10 mice) within 1 mo. However, dermatitis was not observed after the transfer of separated $CD4^+$ or $CD8^+$ cells alone. These results suggest that both $CD4^+$ Th1 and $CD8^+$ Tc1 cells may be active as effector cells in CHS responses in this model. Furthermore, it is known that activated cells produce IFN-γ to activate skin resident cells, which produce cytokines and chemokines allowing the recruitment of the polymorphonuclear cell infiltrates characteristic of CHS. This effector phase of CHS takes

24 to 48 h in the mouse (12), coinciding closely with our results on 24- and 48-h DNFB hyperresponsiveness.

In contrast to T-bet, GATA-3 is known as a Th2 lineage commitment transcription factor (35, 36). We have previously shown that GATA-3 overexpression in Th1-dominant autoimmune disease can diminish autoimmune nephritis (20, 37) and, therefore, that therapy to regulate expression levels of transcriptional factors may be useful to control unbalanced Th1/Th2 activity in many diseases. The results of the present study also suggest that to control Th1 and Tc1 reactions via down-regulation of T-bet expression might be useful for alleviating contact dermatitis.

In conclusion, we have generated Th1- and Tc1-dominant mice that developed spontaneous skin inflammation very similar to contact dermatitis. These mice should be useful for revealing a link between some immune diseases and Th1/Th2 and Tc1/Tc2 dysbalance and may offer a valuable murine model of contact dermatitis.

Acknowledgment

We express our sincere thanks to Laurie H. Glimcher for providing us with mouse T-bet cDNA.

Disclosures

The authors have no financial conflict of interest.

References

1. Mosmann, T. R., H. Cherwinski, M. W. Bond, M. A. Giedlin, and R. L. Coffman. 1986. Two types of murine helper T cell clone. I. Definition according to profiles of lymphokine activities and secreted proteins. *J. Immunol.* 136: 2348–2357.
2. Romagnani, S. 1991. Human TH1 and TH2 subsets: doubt no more. *Immunol. Today* 12: 256–257.
3. Farrar, J. D., H. Asnagli, and K. M. Murphy. 2002. T helper subset development: roles of instruction, selection, and transcription. *J. Clin. Invest.* 109: 431–435.
4. Croft, M., L. Carter, S. L. Swain, and R. W. Dutton. 1994. Generation of polarized antigen-specific CD8 effector populations: reciprocal action of interleukin (IL)-4 and IL-12 in promoting type 2 versus type 1 cytokine profiles. *J. Exp. Med.* 180: 1715–1728.
5. Sad, S., R. Marcotte, and T. R. Mosmann. 1995. Cytokine-induced differentiation of precursor mouse $CD8^+$ T cells into cytotoxic $CD8^+$ T cells secreting Th1 or Th2 cytokines. *Immunity* 2: 271–279.
6. Glimcher, L. H., M. J. Townsend, B. M. Sullivan, and G. M. Lord. 2004. Recent developments in the transcriptional regulation of cytolytic effector cells. *Nat. Rev. Immunol.* 4: 900–911.
7. Szabo, S. J., S. T. Kim, G. L. Costa, X. Zhang, C. G. Fathman, and L. H. Glimcher. 2000. A novel transcription factor, T-bet, directs Th1 lineage commitment. *Cell* 100: 655–669.
8. Sullivan, B. M., A. Juedes, S. J. Szabo, M. von Herrath, and L. H. Glimcher. 2003. Antigen-driven effector CD8 T cell function regulated by T-bet. *Proc. Natl. Acad. Sci. USA* 100: 15818–15823.
9. Lighvani, A. A., D. M. Frucht, D. Jankovic, H. Yamane, J. Aliberti, B. D. Hissong, B. V. Nguyen, M. Gadina, A. Sher, W. E. Paul, and J. J. O'Shea. 2001. T-bet is rapidly induced by interferon-γ in lymphoid and myeloid cells. *Proc. Natl. Acad. Sci. USA* 98: 15137–15142.
10. Afkarian, M., J. R. Sedy, J. Yang, N. G. Jacobson, N. Cereb, S. Y. Yang, T. L. Murphy, and K. M. Murphy. 2002. T-bet is a STAT1-induced regulator of IL-12R expression in naïve $CD4^+$ T cells. *Nat. Immunol.* 3: 549–557.
11. Kimber, I., D. A. Basketter, G. F. Gerberick, and R. J. Dearman. 2002. Allergic contact dermatitis. 2002. *Int. Immunopharmacol.* 2: 201–211.
12. Saint-Mezard, P., F. Bérard, B. Dubois, D. Kaiserlian, and J. F. Nicolas. 2004. The role of $CD4^+$ and $CD8^+$ T cells in contact hypersensitivity and allergic contact dermatitis. *Eur. J. Dermatol.* 14: 131–138.
13. Kimber, I., and R. J. Dearman. 2002. Allergic contact dermatitis: the cellular effectors. *Contact Dermatitis* 46: 1–5.
14. Traidl, C., H. F. Merk, A. Cavani, and N. Hunzelmann. 2000. New insights into the pathomechanisms of contact dermatitis by the use of transgenic mouse models. *Skin Pharmacol. Appl. Skin Physiol.* 13: 300–312.
15. Hauser, C. 1990. Cultured epidermal Langerhans cells activate effector T cells for contact sensitivity. *J. Invest. Dermatol.* 95: 436–440.
16. Kondo, S., S. Beissert, B. Wang, H., Fujisawa, F. Kooshesh, A. Stratigos, R. D. Granstein, T. W. Mak, and D. N. Sauder. 1996. Hyporesponsiveness in contact hypersensitivity and irritant contact dermatitis in CD4 gene targeted mouse. *J. Invest. Dermatol.* 106: 993–1000.
17. Wang, B., H. Fujisawa, L. Zhuang, I. Freed, B. G. Howell, S. Shahid, G. M. Shivji, T. W. Mak, and D. N. Sauder. 2000. $CD4^+$ Th1 and $CD8^+$ type 1 cytotoxic T cells both play a crucial role in the full development of contact hypersensitivity. *J. Immunol.* 165: 6783–6790.
18. Kehren, J., C. Desvignes, M. Krasteva, M. T. Ducluzeau, O. Assossou, F. Horand, M. Hahne, D. Kägi, D. Kaiserlian, and J. F. Nicolas. 1999. Cytotoxicity is mandatory for $CD8^+$ T cell-mediated contact hypersensitivity. *J. Exp. Med.* 189: 779–786.
19. Zhumabekov, T., P. Corbella, M. Tolaini, and D. Kioussis. 1995. Improved version of a human CD2 minigene based vector for T cell-specific expression in transgenic mice. *J. Immunol. Methods* 185: 133–140.
20. Yoh, K., K. Shibuya, N. Morito, T. Nakano, K. Ishizaki, H. Shimohata, M. Nose, S. Izui, A. Shibuya, A. Koyama, et al. 2003. Transgenic overexpression of GATA-3 in T lymphocytes improves autoimmune glomerulonephritis in mice with a BXSB/MpJ-*Yaa* genetic background. *J. Am. Soc. Nephrol.* 14: 2494–2502.
21. Garrigue, J. L., J. F. Nicolas, R. Fraginals, C. Benezra, H. Bour, and D. Schmitt. 1994. Optimization of the mouse ear swelling test for in vivo and in vitro studies of weak contact sensitizers. *Contact Dermatitis* 30: 231–237.
22. Liblau, R. S., S. M. Singer, H. O. and McDevitt. 1995. Th1 and Th2 $CD4^+$ T cells in the pathogenesis of organ-specific autoimmune diseases. *Immunol. Today* 16: 34–38.
23. Snapper, C. M., and J. J. Mond. 1993. Towards a comprehensive view of immunoglobulin class switching. *Immunol. Today* 14: 15–17.
24. Snapper, C. M., F. D. Finkelman, and W. E. Paul. 1988. Differential regulation of IgG1 and IgE synthesis by interleukin 4. *J. Exp. Med.* 167: 183–196.
25. Carroll, J. M., T. Crompton, J. P. Seery, and F. M. Watt. 1997. Transgenic mice expressing IFN-γ in the epidermis have eczema, hair hypopigmentation, and hair loss. *J. Invest. Dermatol.* 108: 412–422.
26. Wang, L. F., J. T. Wu, and C. C. Sun. 2002. Local but not systemic administration of IFN-γ during the sensitization phase of protein antigen immunization suppress Th2 development in a murine model of atopic dermatitis. *Cytokine* 19: 147–152.
27. Akiyama, M., M. Yokoyama, M. Katsuki, S. Habu, and T. Nishikawa. 1993. Lymphocyte infiltration of the skin in transgenic mice carrying the human interleukin-2 gene. *Arch. Dermatol. Res.* 285: 379–384.
28. Turksen, K., T. Kupper, L. Degenstein. I. Williams, and E. Fuchs. 1992. Interleukin 6: insights to its function in skin by overexpression in transgenic mice. *Proc. Natl. Acad. Sci. USA* 89: 5068–5072.
29. Rich, B. E., J. Campos-Torres, R. I. Tepper, R. W. Moreadith, and P. Leder. 1993. Cutaneous lymphoproliferation and lymphomas in interleukin 7 transgenic mice. *J. Exp. Med.* 177: 305–316.
30. Cruz, P. D., Jr. 1996. Basic science answers to questions in clinical contact dermatitis. *Am. J. Contact Dermat.* 7: 47–52.
31. Lu, B., C. Ebensperger, Z. Dembic, Y. Wang, M. Kvatyuk, T. Lu, R. L. Coffman, S. Pestka, and P. B. Rothman. 1998. Targeted disruption of the interferon-γ receptor 2 gene results in severe immune defects in mice. *Proc. Natl. Acad. Sci. USA* 95: 8233–8238.
32. Berg, D. J., M. W. Leach, R. Kühn, K. Rajewsky, W. Müller, N. J. Davidson, and D. Rennick. 1995. Interleukin 10 but not interleukin 4 is a natural suppressant of cutaneous inflammatory responses. *J. Exp. Med.* 182: 99–108.
33. Asada, H., J. Linton, and S. I. Katz. 1997. Cytokine gene expression during the elicitation phase of contact sensitivity: regulation by endogenous IL-4. *J. Invest. Dermatol.* 108: 406–411.
34. Carter, L. L., and R. W. Dutton. 1996. Type 1 and Type 2: a fundamental dichotomy for all T-cell subsets. *Curr. Opin. Immunol.* 8: 336–342.
35. Ting, C. N., M. C. Olson, K. P. Barton, and J. M. Leiden. 1996. Transcription factor GATA-3 is required for development of the T-cell lineage. *Nature* 384: 474–478.
36. Zheng, W., and R. A. Flavell. 1997. The transcritpion factor GATA-3 is necessary and sufficient for Th2 cytokine gene expression in CD4 T cells. *Cell* 89: 587–596.
37. Takahashi, S., L. Fossati, M. Iwamoto, R. Merino, R. Motta, T. Kobayakawa, and S. Izui. 1996. Imbalance towards Th1 predominance is associated with acceleration of lupus-like autoimmune syndrome in MRL mice. *J. Clin. Invest.* 97: 1597–1604.